CHAPTER - 3

*Sulphide thin films prepared by the dip technique

3. INTRODUCTION

Sulphide thin films are extensively used for the fabrication of a number of solid state devices such as solar cells, photoconductive cells, electroluminescent cells, Schottky diode, thin film transistors etc. A large variety of deposition techniques (discussed in chapter 1) have been used for the preparation of these films. Efforts are under way to develop simple and low-cost methods for the deposition of sulphide films for use in various device applications, especially in solar cells.

Results obtained under various deposition conditions are by no means unique. Different workers have reported different results even under similar deposition conditions.

The dip technique is a simple method for the deposition of device-quality sulphide films. This technique is traditionally used for deposition of oxide films as described in chapter 2, where a solution of corresponding metal chloride in an organic solvent is used as the starting solution. In case of sulphide film preparation, it has been observed that simple addition of a suitable sulphur containing compound to the starting solution prepared originally for the oxide film deposition results in a good quality sulphide film.

In this chapter, we describe the deposition of a number of binary and ternary sulphide films by the dip technique and their characterisation.

*3.1. $Zn_xCd_{1-x}S$ THIN FILMS

3.1.1. INTRODUCTION

Ternary sulphide compounds are some of the most promising man-made materials since they yield new possibilities for tailoring physical properties. Among them the wide band-gap II-VI compound semiconductors have found application in optoelectronic devices. There have been attempts to introduce $Zn_xCd_{1-x}S$ alloy layers instead of CdS for obtaining specific band structure and optical properties [1] for use in solar cells.

These films have been widely used as a wide bandgap window material in heterojunction photovoltaic solar cells [2-7], and in photoconductive devices [8]. In solar cell systems, where CdS thin films have been proved to be useful, partial substitution of Zn for Cd increases the optical window of the heterojunction and also the diffusion potential [9]. Moreover, in heterojunction solar cells using $CuGaSe_2$, use of $Zn_xCd_{1-x}S$ instead of CdS can lead to an increase in photocurrent by providing a match in the electron affinities of the two materials. This hexagonal $Zn_xCd_{1-x}S$ ternary compound is also potentially useful as a window material for fabrication of p-n junctions without lattice mismatch in the devices based on quaternary materials like $CuIn_xGa_{1-x}Se_2$ [10] or $CuIn(S_zSe_{1-z})_2$ [11].

Zn $_xCd_{1-x}S$ thin films have been prepared by a variety of techniques, which include vacuum evaporation [12-13], spray pyrolysis [14-16], rf sputtering [17], solution growth [18-19] and sublimation growth [20]. Metal-organic vapour-phase epitaxy (MOVPE) [21] and molecular-beam epitaxy (MBE) [22] have been recently applied to prepare these films for the fabrication of efficient light-emitting devices.

---

* **Published in the "journal of Thin Solid Films" Vol. 322/1-2 (1998) P. 117-122.**

Ion-beam deposition method makes it possible to fabricate high-quality ZnCdS films at a low substrate temperature without interdiffusion in multilayers and heterojunction devices [23, 25].

As discussed previously (chapter 2), the dip technique and the related sol-gel method have been traditionally used for the deposition of oxide thin films [26-27]. Usually these involve the hydrolysis of the corresponding metal alkoxide, nitrate or chloride on a heated substrate. Previous workers [28] reported a modification of the dip technique for deposition of sulphide films. In this method the substrate is withdrawn from an alcoholic solution of the metal nitrate and thiourea, and with the liquid layer adhering to it, transferred to a furnace maintained at a high temperature. A chemical reaction then takes place on the substrate to yield the solid sulphide films.

As described in ref. [28], attempts to produce $Cd_{0.8}Zn_{0.2}S$ films using a starting solution containing both cadmium and zinc nitrates resulted in the formation of a mixed phase material containing partially crystalline CdS and amorphous ZnS when prepared at a baking temperature of 400° C and baking time (B_T) five minutes. We have found that by increasing the baking temperature to 500° C (B_T = 5 minutes) homogeneous crystalline $Zn_xCd_{1-x}S$ films within the range $0 \leq x \leq 0.6$ could be produced. These films show a continuous variation of lattice parameter and bandgap as a function of atomic fraction x within the range $0 \leq x \leq 0.6$. For $x > 0.6$, the films tend to develop an amorphous character, but the optical properties are not affected and the bandgap varies monotonically from 2.3eV (CdS) to 2.69 eV ($Zn_{0.6}Cd_{0.4}S$) over the range $0 \leq x \leq 0.6$. In this chapter, the preparation of these films and their characterization by x-ray diffractometry, scanning electron microscopy, optical and photoconductivity measurments have been described.

3.1.2. EXPERIMENTAL DETAILS

3.1.2.1. SOLUTION PREPARATION

Three separate saturated solutions of cadmium nitrate [$Cd(NO_3)_2$, $4H_2O2$], zincnitrate [$Zn(NO_3)_2$, $6H_2O$] and thiourea with methanol as solvent were initially prepared. The concentrations are 0.8 kg/litre, 1.0 kg/litre and 0.1 kg/litre respectively. They were then mixed in requisite amounts to prepare the starting solution for deposition of sulphide films. It was observed that the mixing was best achieved without any precipitation taking place if the thiourea solution was initially divided into two parts which were mixed with the two nitrate solutions separately, and finally one of the mixtures slowly added to the other.

3.1.2.2. FILM FORMING PROCESS

Microscope glass-slides were usually used as a substrate. These were cleaned by washing in detergent solution and chromic acid and finally degreased in acetone and methanol vapour. The film forming process is exactly the same as described in chapter 2 for oxide films, which involves dipping of the substrate in the starting solution, its withdrawal at a controlled speed and transfer to a furnace for baking for almost 5 minutes. The chemical reactions for CdS and ZnS films are as follows.

$$Zn(NO_3)_2 + (NH_2)_2CS = ZnS + CO_2 + 2H_2O + 2N_2O \text{ ---------- (3.1)}$$

$$Cd(NO_3)_2 + (NH_2)_2CS = CdS + CO_2 + 2H_2O + 2N_2O \text{ ---------- (3.2)}$$

The minimum baking temperature required for the deposition of a solid films was found to be 300° C. It was observed that single phase crystalline films of a very high quality were obtained when prepared at a baking temperature of 500° C for five

minutes baking time. Thickness of the films could be increased by repeating the whole cycle (dip-withdrawal-bake) a number of times. All the films reported here were baked for a fixed baking time of five minutes within the furnace under atmospheric conditions.

3.1.3. RESULTS AND DISCUSSION

$Zn_xCd_{1-x}S$ films were deposited at 500° C for various concentrations of Zn from x = 0 to x = 1. The value of x was changed by changing the relative concentrations of Zn - nitrate and Cd - nitrate in the starting solution. The $Zn_xCd_{1-x}S$ thin films were smooth, highly uniform, reflecting and strongly adherent to the substrate. Colour of the films was observed to change from yellow-orange to pale yellow with increase in zinc atomic fraction x. Zinc sulphide films (x=1) were white in colour while cadmium sulphide films (x=0) were orange-yellow in colour. Characterization of the films was carried out by optical absorption, X-ray diffractometry, scanning microscopy and spectral response of photo conductivity measurements. Results reported in this chapter were obtained by measurements on films prepared by 10 dippings (dip-withdrawal-bake cycle) from a starting solution containing total 0.93 (Cd + Zn) moles per litre and withdrawn at a speed of 1.33 mm/sec and baked at 500° C for five minutes.

The Zn/Cd ratio in the solid films was determined by Atomic Absorption Spectroscopy. The value of x was found to be essentially the same as the relative proportion of Zn atoms [Zn:(Zn+Cd)] in the starting solution.

3.1.3.1. FILM THICKNESS

Films of different thickness were obtained by changing the lifting speed as well as increasing the number of dippings (dip-withdrawal-bake cycle), keeping the concentration of the solution fixed. Smooth and uniform films could be obtained upto a maximum withdrawal speed of 1.33 mm / sec. For higher speeds, the films tended to be non-uniform. As discussed in chapter 2, at high withdrawal speeds the liquid layer adhering to the substrate, as it is pulled out is quite thick, and turbulence in this layer is also higher. Film thickness was measured by stylus method using α step as described in chapter 2.

Figure 3.1 shows the variation of the thickness of the films for different values of x, when the total number of (Cd + Zn) moles were kept constant in a given volume of the starting solution. It shows that the thickness of the films decreased linearly with the increase in zinc proportion.

3.1.3.2. X-RAY DIFFRACTOMETRIC STUDY

X-ray diffractometry studies were carried out by PHILIPS diffractometer (model PW 1390) with CuK_{α} radiation (Ni-filter) at 1.54 Å. Figure 3.2 shows the XRD patterns of the $Zn_xCd_{1-x}S$ films (x=0.2) deposited at three baking temperatures T_B = 400° C, 500° C and 600° C. It is clear from the diffractograms that the $Zn_xCd_{1-x}S$ films deposited at a baking temperature of 500°C is hexagonal in structure where as that deposited at 400° C is a mixed phase, containing crystalline CdS (cubic) and amorphous ZnS, with a prominent peak at $2\theta = 26.87°$ (d-value 3.32 Å) coresponding to (111) plane of CdS. No prominent peaks were observed in the film deposited at a baking temperature of 600° C.

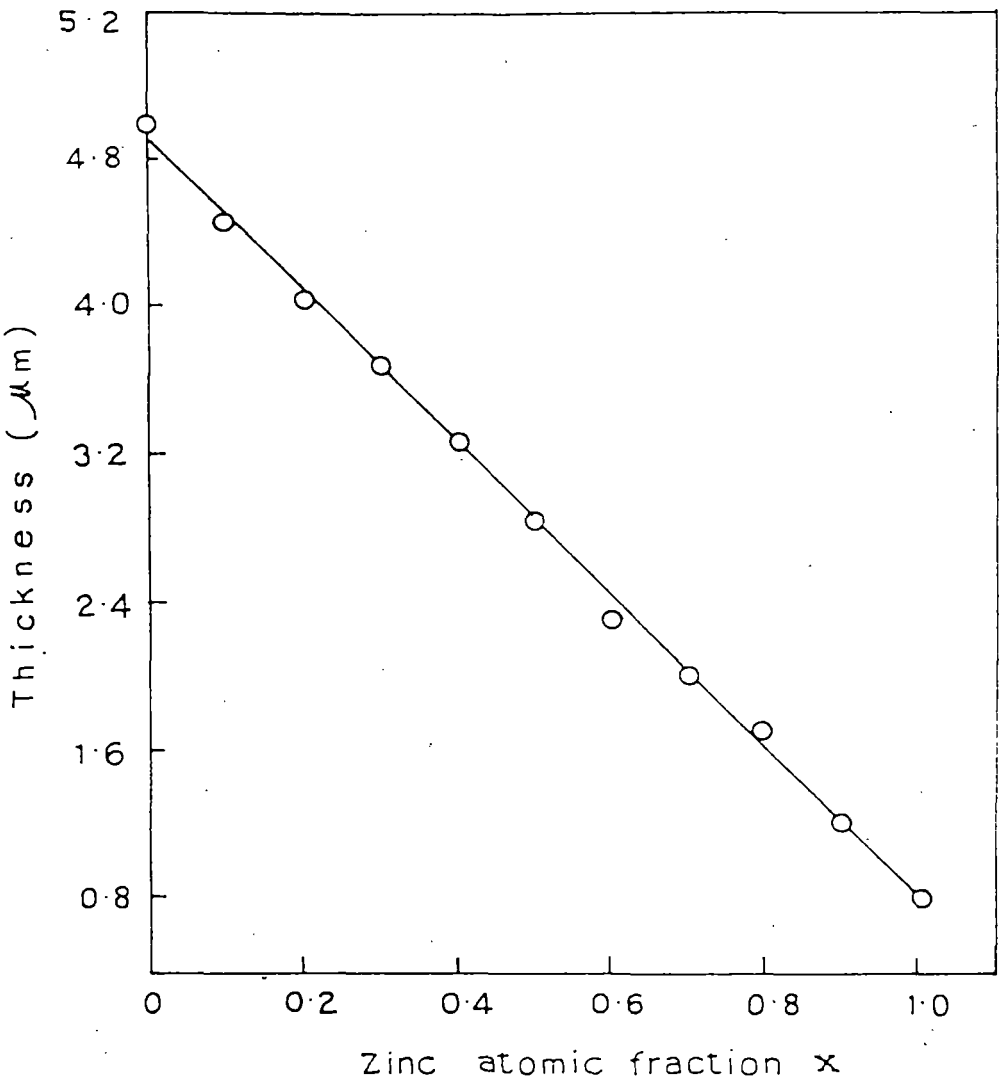

Figure 3.1. Variation of thickness on zinc atomic fraction x of $Zn_xCd_{1-x}S$ thin films ($T_B = 500^o$ C).

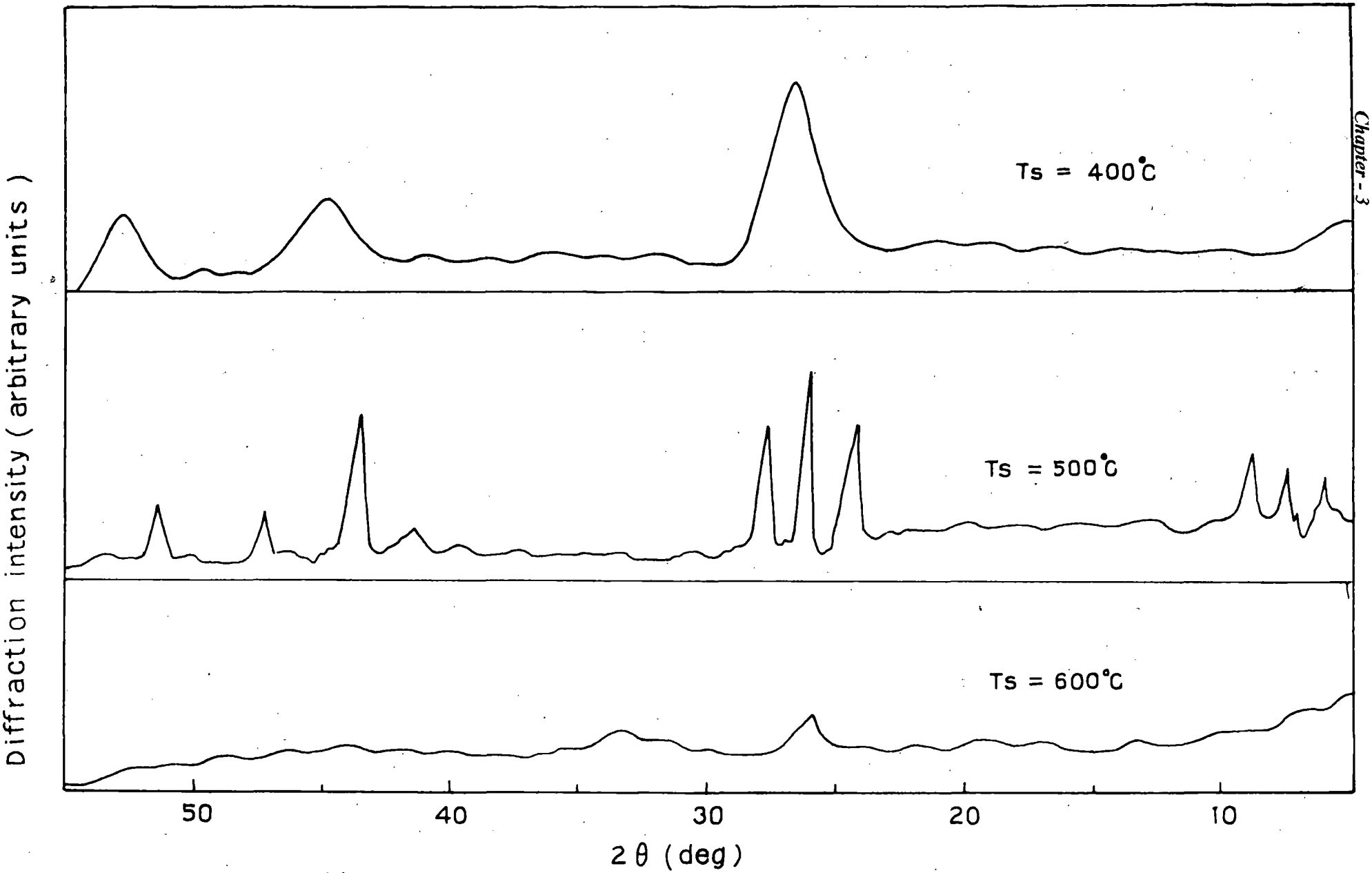

Figure 3.2. X-ray diffractograms of $Zn_xCd_{1-x}S$ (x = 0.2) thin films at various baking temperatures (T_B = 400° C, 500° C, 600° C).

As films with best crystalline properties were obtained for a baking temperature 500° C and a baking time of five minutes, these films were chosen for further detailed study of their properties as a function of atomic fraction x.

In the compositional range $0 \leq x \leq 1$, the crystal structure of the $Zn_xCd_{1-x}S$ films have been determined from x-ray diffraction patterns. The analysis established the presence of hexagonal structure of the polycrystalline $Zn_xCd_{1-x}S$ films in the range $0 \leq x \leq 0.6$. Films with composition corresponding to $x > 0.6$ was found to be nearly amorphous in nature.

A typical XRD pattern for $Zn_xCd_{1-x}S$ (for $x=0.4$) films is shown in figure 3.3. Comparison of the prominent peak position (2θ–value) of the XRD spectra with the JCPDS data file for CdS [29] suggests that the $Zn_xCd_{1-x}S$ film deposited at a baking temperature of 500° C is hexagonal (wurtzite) in structure with the prominent x-ray diffraction peaks corresponding to (100), (002), (101), (110) and (103) planes.

It is observed that the diffraction angle (2θ) shifts to higher angles with increasing zinc atomic fraction x. The peaks, which are quite sharp upto $x = 0.4$, become weaker beyond this and no prominent peaks appear for $x > 0.6$, which means that in this range the films are mostly amorphous.

The diffraction angle shifts towards higher angles with an increase in the composition parameter x, which means that the lattice constant decreases with x. The relationship between the lattice parameter and the zinc atomic fraction x over the range $0 \leq x \leq 0.6$ is shown in figure 3.4. It was observed that the lattice constant decreases with increase in the proportion of Zn. This is consistent with the smaller size of the Zn atoms and also reflected in the decrease in thickness of the films with increasing x as described in section 3.3.1. Similar results were obtained by Yamaquchi et al. [30]. The values of a and c for thin film prepared at $x = 0$ (pure CdS) are 4.13 Å and 6.73 Å respectively. These values are in good agreement with the data for hexagonal CdS films from the JCPDS card [29].

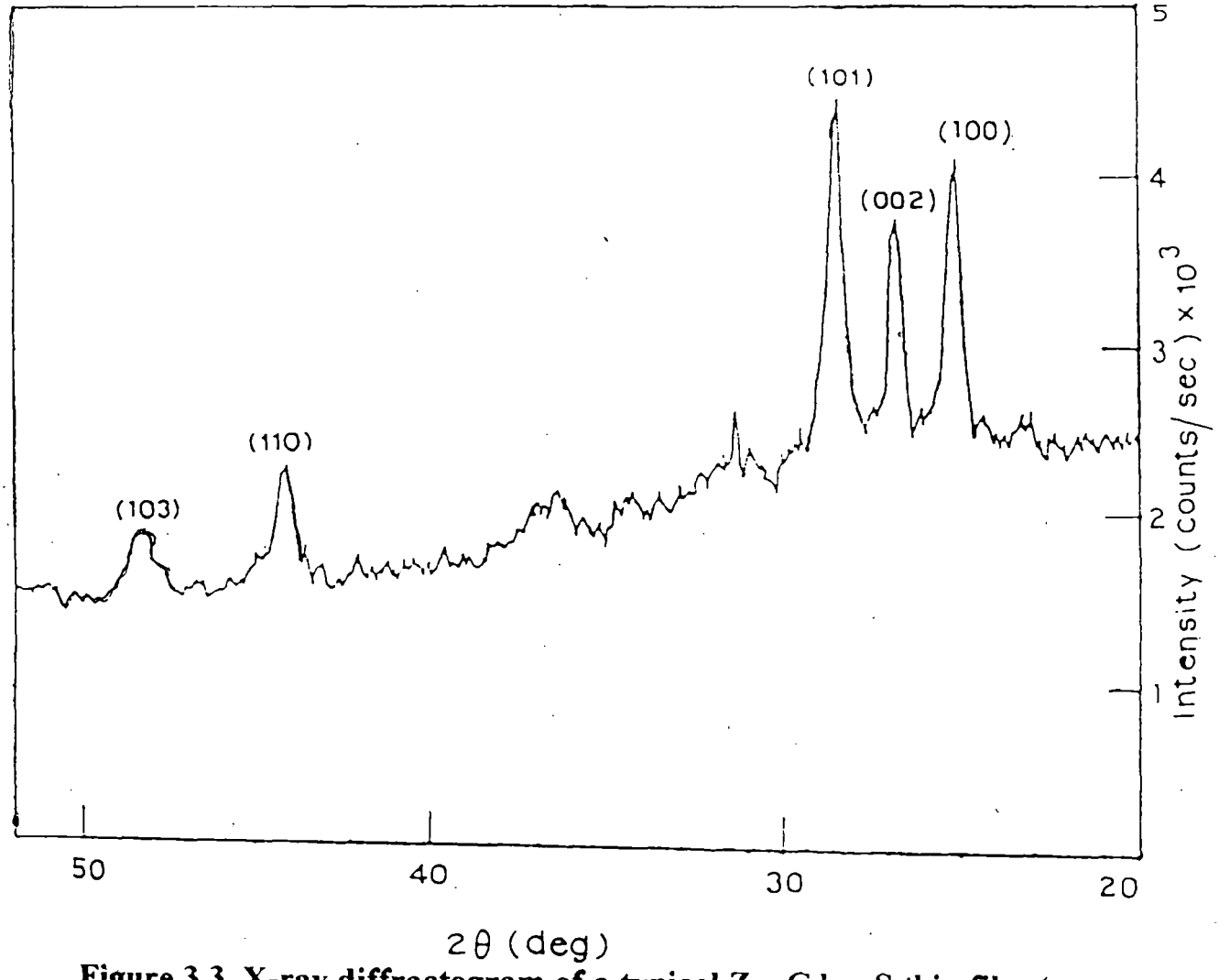

Figure 3.3. X-ray diffractogram of a typical $Zn_xCd_{1-x}S$ thin film (x= 0.4) deposited on glass substrate at 500° C.

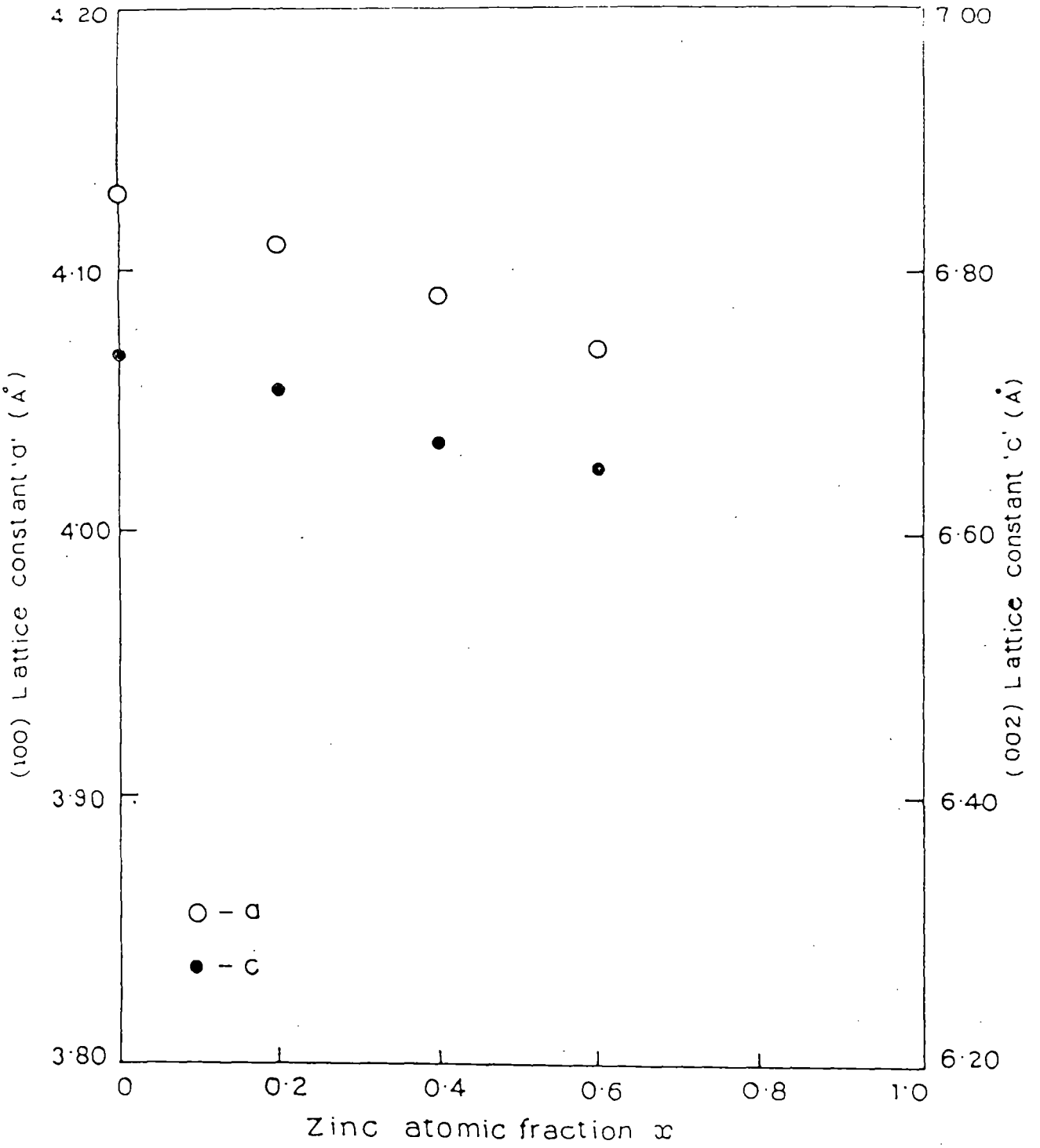

Figure 3.4. Dependence of the lattice constants *c* and *a* on zinc atomic fraction x.

X-ray diffraction of a typical $Zn_xCd_{1-x}S$ film (x= 0.4) deposited at a baking temperature of 500° C upon a dip-deposited polycrystalline CdS film with hexagonal structure is shown in figure 3.5. The underlying CdS thin film of thickness ~ 0.3 μ was deposited initially by the dip technique on crystalline tin-dioxide transparent conducting substrate at a temperature of 500° C. The top layer of $Zn_xCd_{1-x}S$ film (x=0.4) of thickness 0.9 μ was deposited on the CdS. The deposited film is also has a much and more pronounced peak, indicating a higher order of crystallinity and is also hexagonal in structure with preffered orientation along (002) plane.

3.1.3.3. OPTICAL PROPERTIES

3.1.3.3.1. Optical absorption

Optical properties were studied by SHIMADZU UV-240 double-beam spectrophotometer. Optical absorption spectra of $Zn_xCd_{1-x}S$ ($0 \leq x \leq 1$) thin films deposited on glass substrates were obtained in the range 350 nm - 600 nm. (Fig.3.6). The spectra were taken with respect to the bare substrate placed in the reference beam. The absorption edges are quite sharp, indicating that the films are uniform and homogeneous, and these move towards shorter wavelength with increasing Zn atomic fraction x corresponding to increasing bandgap of the material. The optical energy gap (E_g) of the $Zn_xCd_{1-x}S$ thin film was estimated by measuring optical density (O.D) of the films as a function of wavelength in the range 2.2 eV to 3.5 eV, from which absorption co-efficient (α) was obtained. Plots of $(\alpha h\nu)^2$ and $(\alpha h\nu)^{1/2}$ against $h\nu$ were made (Figure 3.7). $(\alpha h\nu)^2$ versus $h\nu$ plots yielded straight line over the range $0 \leq x \leq 0.6$. In contrast, for $x > 0.6$ straight lines were obtained when $(\alpha h\nu)^{1/2}$ was plotted against $h\nu$. This is indicative of the fact that the film are crystalline for $0 \leq x \leq 0.6$ and amorphous beyond this range. The bandgap of hexagonal $Zn_xCd_{1-x}S$ films obtained for the range $0 \leq x \leq 0.6$, using the curve

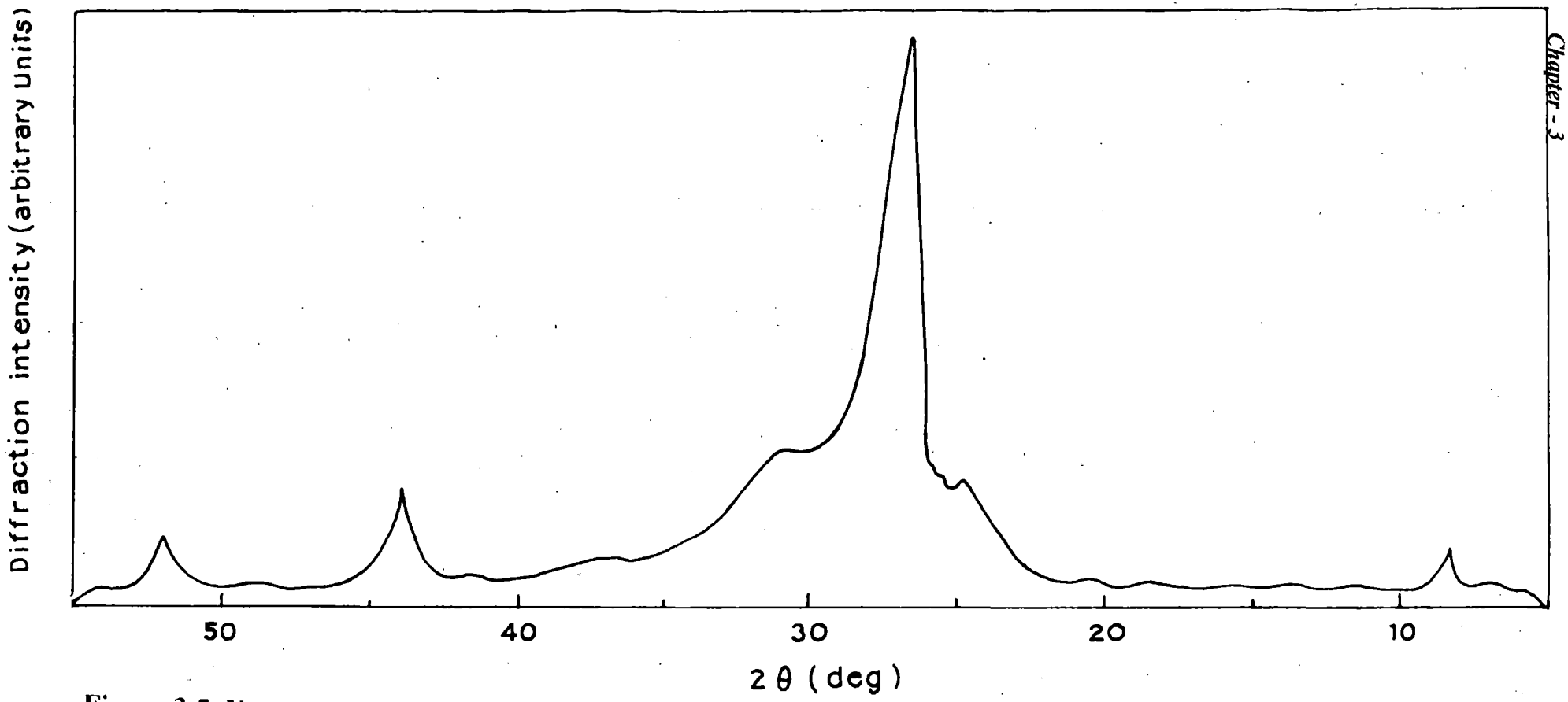

Figure 3.5. X-ray diffractogram of a typical $Zn_xCd_{1-x}S$ thin film (x= 0.4) deposited on a polycrystalline SnO_2-CdS film a 500° C.

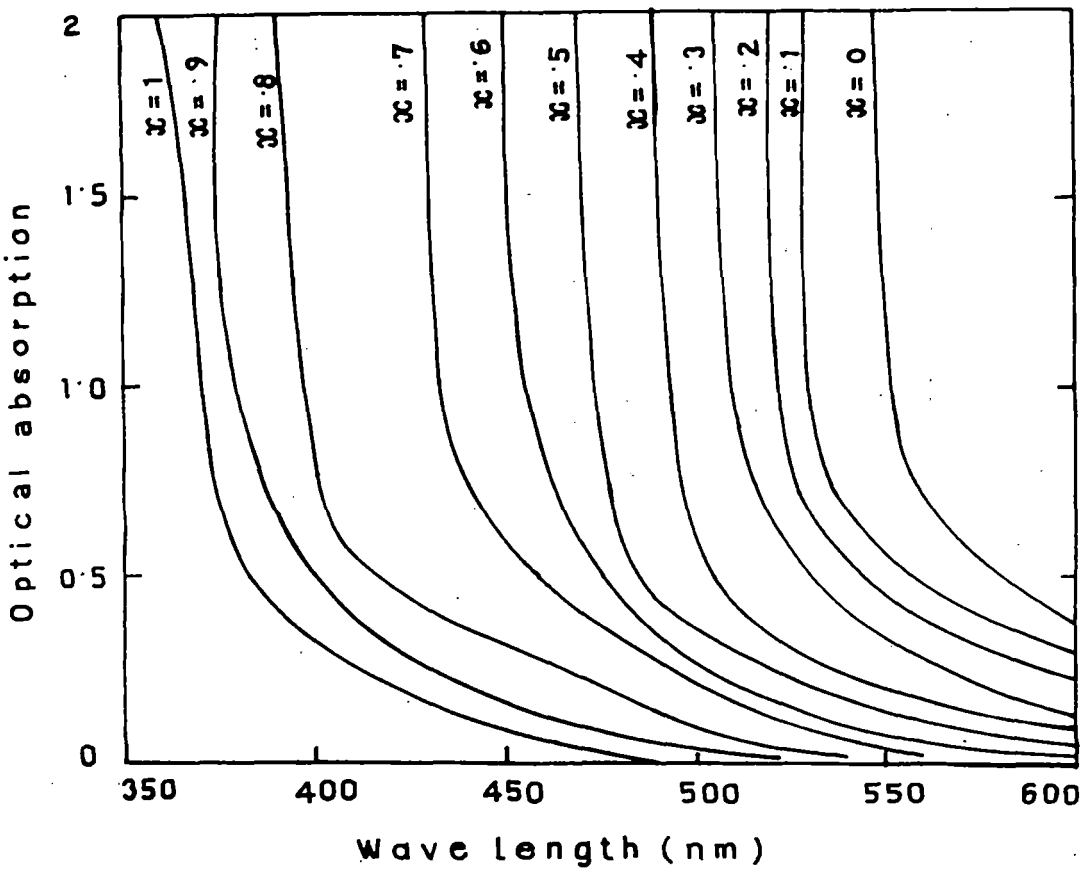

Figure 3.6. Optical absorption spectra of $Zn_xCd_{1-x}S$ ($0 \leq x \leq 1$) thin films.

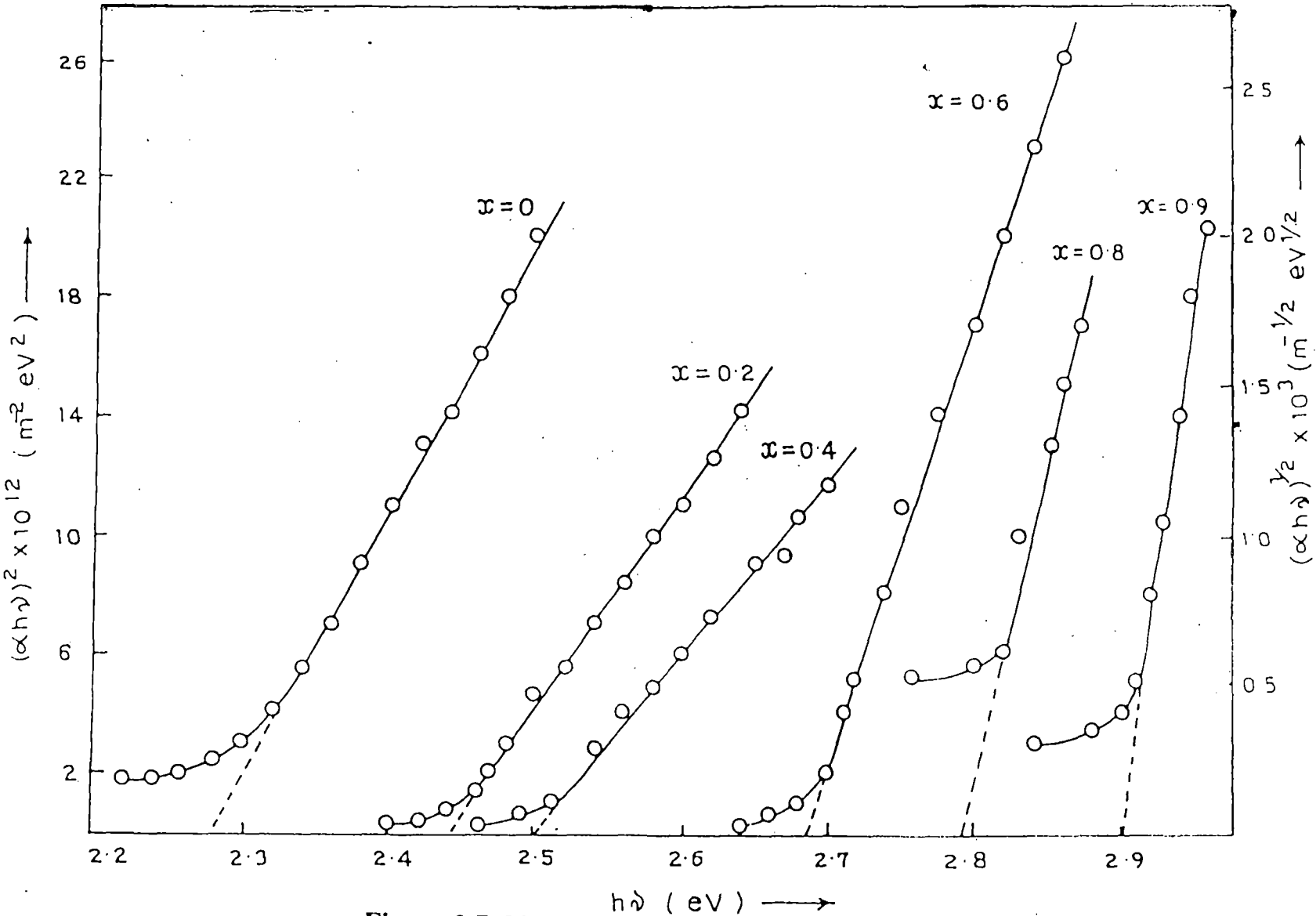

Figure 3.7. Plots of $(\alpha h\nu)^2$ and $(\alpha h\nu)^{1/2}$ against hν curves for $Zn_xCd_{1-x}S$ ($0 \le x \le 1$) thin films.

$(\alpha h\nu)^2$ versus $h\nu$ are in good agreement with other bandgap data obtained from the films deposited by spray pyrolysis [31] or Electron Beam Epitaxy [32].

In the above α was estimated by the following relation.

$$\alpha = \frac{(2.303)X(O.D)}{d} \text{--------(3.3)}$$

where 'd' is the film thickness and O.D. is the optical density, which was converted into transmittance according to the relation given below.

$$O.D. = \log_{10}\left(\frac{I_o}{I}\right) \text{--------(3.4)}$$

and

$$T = \frac{I}{I_o} \text{--------(3.5)}$$

Where I_0 is the intensity of light incident on the film and I is that transmitted beam.

3.1.3.3.2. Spectral response of photoconductivity

To determine the photoconductive (PC) spectral response, a PC cell was fabricated by depositing Ag-electrodes in the usual interdigitated (comb-like) pattern, which was subsequently placed at the detector position of a SPECTROMOM 202 spectrophotometer, and the photocurrent was measured as function of wavelength. The area of the cell was about one square cm. It is known that deposition of Ag after ionic bombardment at high vacuum as was done in this case, produces an ohmic contact with the underlying surface. The pattern of the cell as well as the circuit used for measurement of photocurrent is shown in figure 3.8.

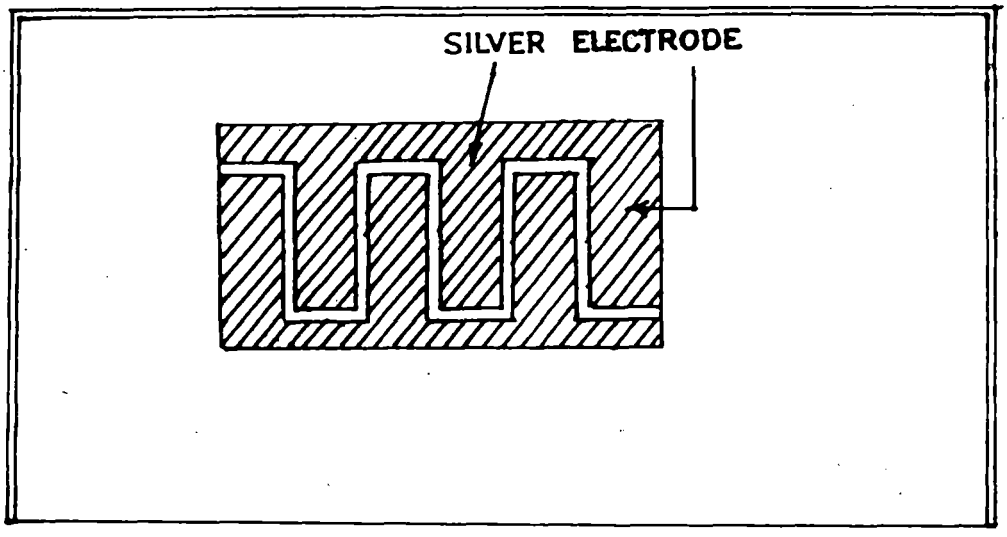

(a)

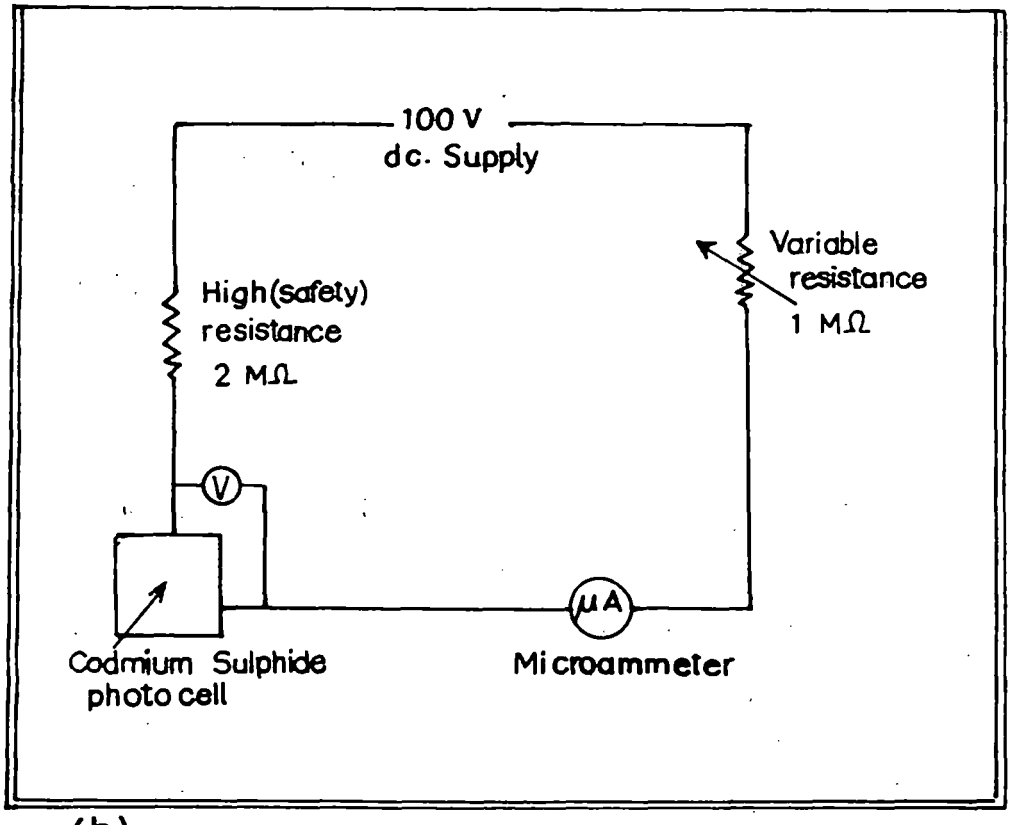

(b)

Figure 3.8. Pattern of the cell and circuit diagram for measurement of photocurrent.

Spectral response of photoconductivity curves are shown in figure 3.9. The photocurrent values are normalized with the peak response for pure CdS taken as 1. No correction was made for the variation of intensity with wavelength of the tungsten filament source used in the spectrophotometer. With increasing x, position of the maximum moves from 540 nm for CdS to 360 nm for ZnS, corresponding to a shift in bandgap from 2.3 eV to 3.4 eV. This continuous change in bandgap with increasing proportion of zinc again confirms the formation of a solid solution.

Figure 3.10 shows the variation with x of (i) bandgap for $0 \leq x \leq 0.6$, (ii) optical gap for $x > 0.6$, and (iii) the photon energy $0 \leq x \leq 1$ at which peak response in photoconductivity is obtained. Curves (i) and (iii) agree quite closely in the range $0 \leq x \leq 0.6$, where crystalline films were obtained. The optical bandgap for $x > 0.6$ are much less than that obtained from photoconductive measurements, which may be due to the amorphous nature of the films in the region.

According to H. Hill [33], the optical bandgap E_x of $Zn_xCd_{1-x}S$ which is a ternary alloy film, can be expressed as

$$E_{(x)} = E_{CdS} + (E_{ZnS} - E_{CdS} - b)x + bx^2 \quad ---(3.6)$$

where b is the bowing parameter and x is the Zn atomic fraction. The value of b for films is about 0.22 eV, estimated from curve fitting with the values of optical bandgap in the range $0 \leq x \leq 0.6$. This value is very close agreement with theory as obtained by Hill [33]. For $x > 0.6$ the value of b changes sharply to 0.07, again indicating a transition from crystalline to amorohous films.

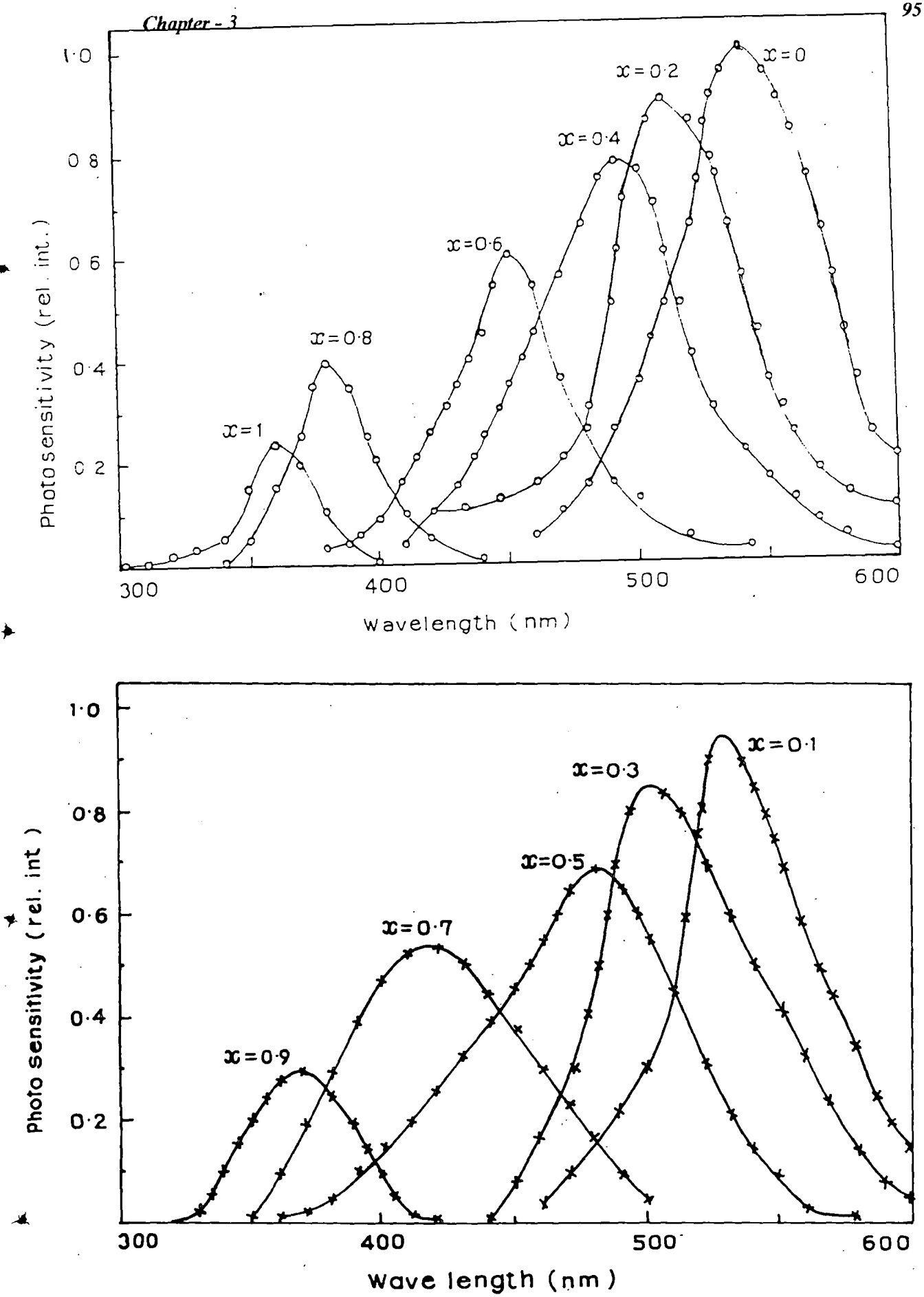

Figure 3.9. Spectral response of photoconductivity curves of $Zn_xCd_{1-x}S$ thin films.

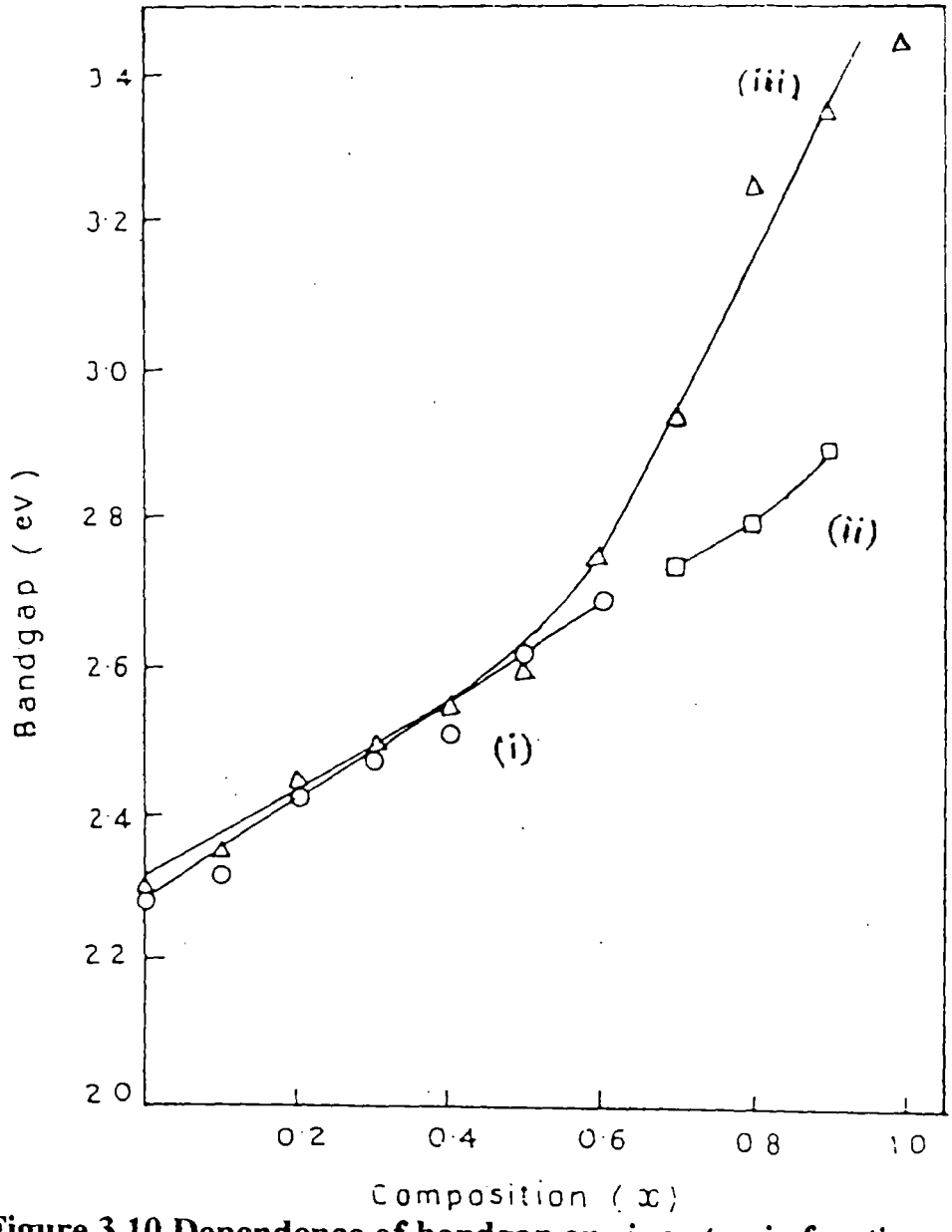

Figure 3.10.Dependence of bandgap on zinc atomic fraction x in $Zn_xCd_{1-x}S$ thin films.

3.1.3.4. SURFACE MORPHOLOGY

Surface morphology studies were carried out by HITACHI S-530 scanning electron microscope. Figure 3.11 shows the SEM micrographs of $Zn_xCd_{1-x}S$ thin films for different values of zinc atomic fraction x. It is evident from the micrographs that the average grain size of the film increases upto x = 0.4, beyond which a tendency of reduction in crystallinity is observed. This is also evidenced in the XRD pattern, where sharp peaks are observed only over the range $0 \leq x \leq 0.4$. The average grain size changes from 0.5 μm (x = 0) to 0.9 μm (x = 0.4), beyond which (x > 0.6) the grains are not properly defined.

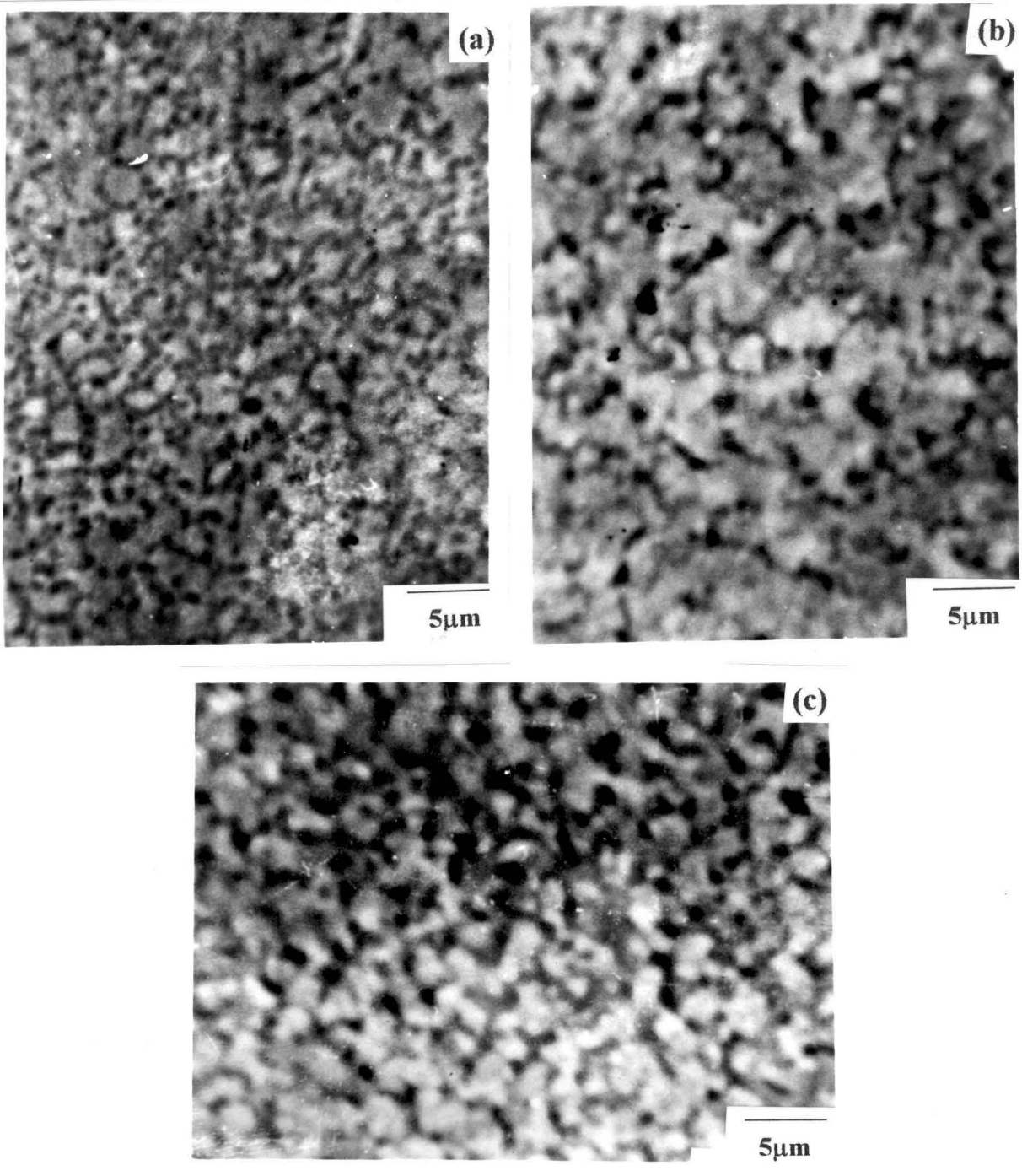

Figure 3.11. Scanning electron micrographs of $Zn_xCd_{1-x}S$ thin films,

(a) X=0, (b) x=0.1, (c) x=0.3.

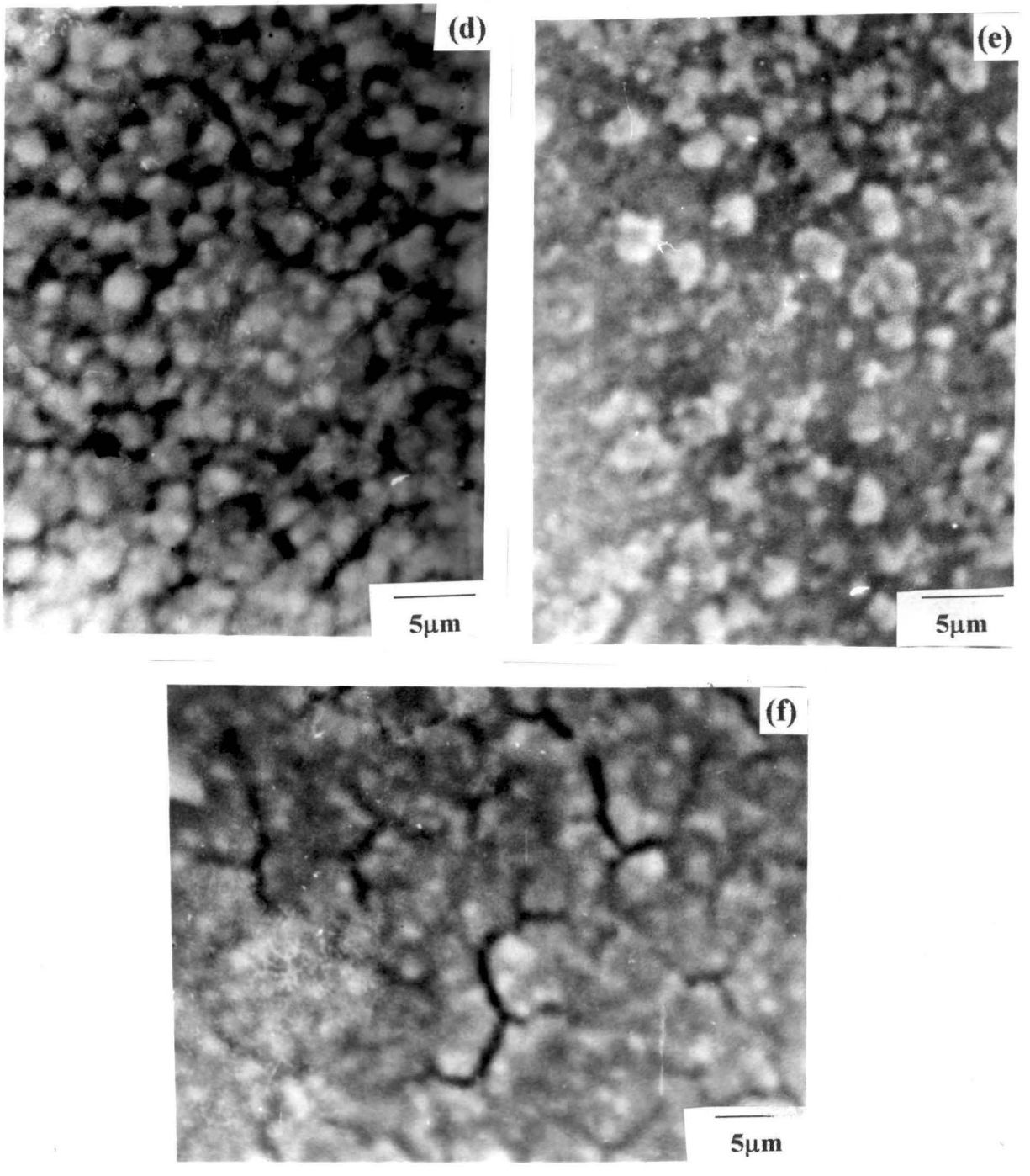

Figure 3.11. Scanning electron micrographs of $Zn_xCd_{1-x}S$ thin films, (d) X=0.4, (e) x=0.5, (f) x=0.6.

*3.2. TIN SULPHIDE (SnS & SnS_2) THIN SOLID FILMS

3.2.1. INTRODUCTION

Efforts have been made currently in finding new materials for energy conversion. Two important factors that should be considered in production of these materials are the band gap energy matching the solar spectrum and the competitiveness of production cost. The first criterion is met by several materials such as Si and GaAs which are being used currently. However, the costs are extremely high for large scale production and can be brought down only by simplifying the manufacturing process.

In the present decade, semiconducting chalcogenide thin films have received much attention because of their world-wide application in the various field of science and technology [34]. In addition, a drastic cut in the cost of production of semiconductor devices is also possible by the use of semiconducting thin films in place of single crystal. Among other materials of recent interest are metal chalcogenides such as CdS and CdSe which fall in the group of II-VI compounds. Among the chalcogenide thin films, tin sulphides show promise because of their possible application in solid state devices, such as photovoltaic [35-38], photoelectrochemical cells (PEC) [39], photoconductive cells [40] and intercalation battery systems [41]. However, compounds of tin sulphide have not been extensively studied.

Tin forms several binary sulphides, such as SnS (orthorhombic) [42-43], SnS_2 (trigonal) [44], Sn_2S_3 (rhombic) [45], and Sn_3S_4 (tetragonal) [46]. All these are semiconducting materials.

---

* **Communicated to the " Thin Solid Films" July 1998.**

Polycrystalline SnS which is usually a p-type semiconductor, with optical and thermal bandgaps of 1.08 eV and 1.20 eV respectively [35-36, 47], may be very interesting for the photovoltaic coversion of solar energy into electrical energy, since its bandgap is comparable to that of silicon [40].

Tin disulphide (SnS_2) is also a very interesting material, both for its layered structure and for the antisotropy of its properties, which makes it a good candidate for utilisation in photochemical solar cells. This compound crystallizes in the CdI_2 type structure with layers of atoms in a close packed arrangement. Within each layer the bonding is mainly covalent, while the layers interact with each other through van der Waals forces. The bandgap of SnS_2 films is about 2.2 eV which is more suitable for photoconductive and photoelectrochemical cells [39-40].

However, comparatively few reports are available for preparation, study and application on these films.

A number of deposition techniques, which include chemical deposition [40,48], evaporation technique [34], chemical vapour transport [49] and electrodeposition [50] have been used for the preparation of these films.

Development of the dip technique for the deposition of SnS and SnS_2 thin films would of practical interest, since dip technique is both simple and economic. An attempt was therefore made to deposit mono and di-sulphides of tin by simple variation of stoichiometry.

These tin sulphide films could be converted easily to tin dioxide by simple annealing in air, thus providing another route for the preparation of transparent conducting tin oxide films.

In this section, we describe in detail the preparation of SnS and SnS_2 films by the dip technique and their characterization by Scanning Electron Microscopy (SEM), X-ray diffractometry (XRD), studies of optical and photoconductive properties, and their conversion to SnO_2 films by air annealing in atmospheric condition.

3.2.2. EXPERIMENTAL DETAILS

Two separate saturated solutions of $SnCl_2.2H_2O$ and thiourea with methanol as solvent were initially prepared. Then they were mixed in requisite amounts together slowly to yield the starting solution for the preparation of SnS and SnS_2 thin films. As a rough guide, 15 gms $SnCl_2.2H_2O$ in 30 cc methanol and 5 gms thiourea in 50 cc methanol was taken for preparation of SnS films whereas for SnS_2 films, 5 gms of more thiourea with 50 cc methanol was added in the above solution .

The films were prepared using the same setup and technique as mentioned in Chapter 2, where speed of withdrawal was 1.33 mm/sec and freshly prepared solutions were used. The films were prepared on soda-glass substrate at different baking temperature in the range 200° C - 360° C for 5 minutes baking time. The formation of SnS and SnS_2 films on the surface of the substrate takes place according to the following reactions.

$$SnCl_2 + (NH_2)_2CS + 2H_2O \rightarrow SnS + 2NH_4Cl + CO_2 \text{ ----(3.7)}$$

To prepare SnS_2 films, a starting solution having $SnCl_2$ and thiourea in 1:2 molar ratio was used and the corresponding equation is given below.

$$SnCl_2 + 2(NH_2)_2CS + 2H_2O \rightarrow SnS_2 + 2NH_4Cl + CO_2 \text{ ----(3.8)}$$

It may be mentioned that the various intermediate chemical reactions and products in the above reactions are quite complex and not known in detail.

SnS and SnS_2 films were deposited at baking temperatures of 200° C, 300° C & 360° C and for a baking time of 5 minutes. Optical absorbtion, photoconductive (PC) spectral response and microstructural studies were carried out using SHIMADZU UV-240 double-beam spectrophotometer, SPECTROMOM 202 spectrophotometer,

PHILIPS diffractometer (model PW 1390) with CuKα radiation (Ni-filter) at 1.54 Å, HITACHI S-530 scanning electron microscope respectively as mentioned earlier (section 4.2). As described earlier, the thickness of the films was measured by stylus method using α step.

SnS and SnS_2 films were baked in a furnace in atmospheric condition at 400° C for different times (10 - 120 minutes) to convert them to transparent conducting tin dioxide film. The SnO_2 films were characterized by XRD, SEM, optical transmission measurements, and variation of their sheet resistance were recorded, using standard four probe method. Optical absorption and doping effects were studied using SnS_2 films only.

3.2.3. RESULTS AND DISCUSSION

Tin mono and di-sulphide films were smooth, shiny and strongly adherent to the substrate. The films were also highly uniform except for the trouble zone at the bottom and sides as described in Chapter 2. The colour of SnS and SnS_2 films was black and golden yellow respectively.

3.2.3.1. THICKNESS

Films of different thickness were obtained by changing multiple dippings. Figure 3.12 shows the thickness variation with number of dippings of SnS_2 films at a baking temperature of 360° C. It is seen that the thickness per dipping is lower for first dip compared with the subsequent dippings. This may be due to the fact that first deposition is on amorphous glass substrate whereas the subsequent depositions are on crystalline SnS_2 layer itself. Similar results were obtained by Karanjai et al. for CdS films [28]. Thickness variation of SnS films with number of dippings follows same nature as

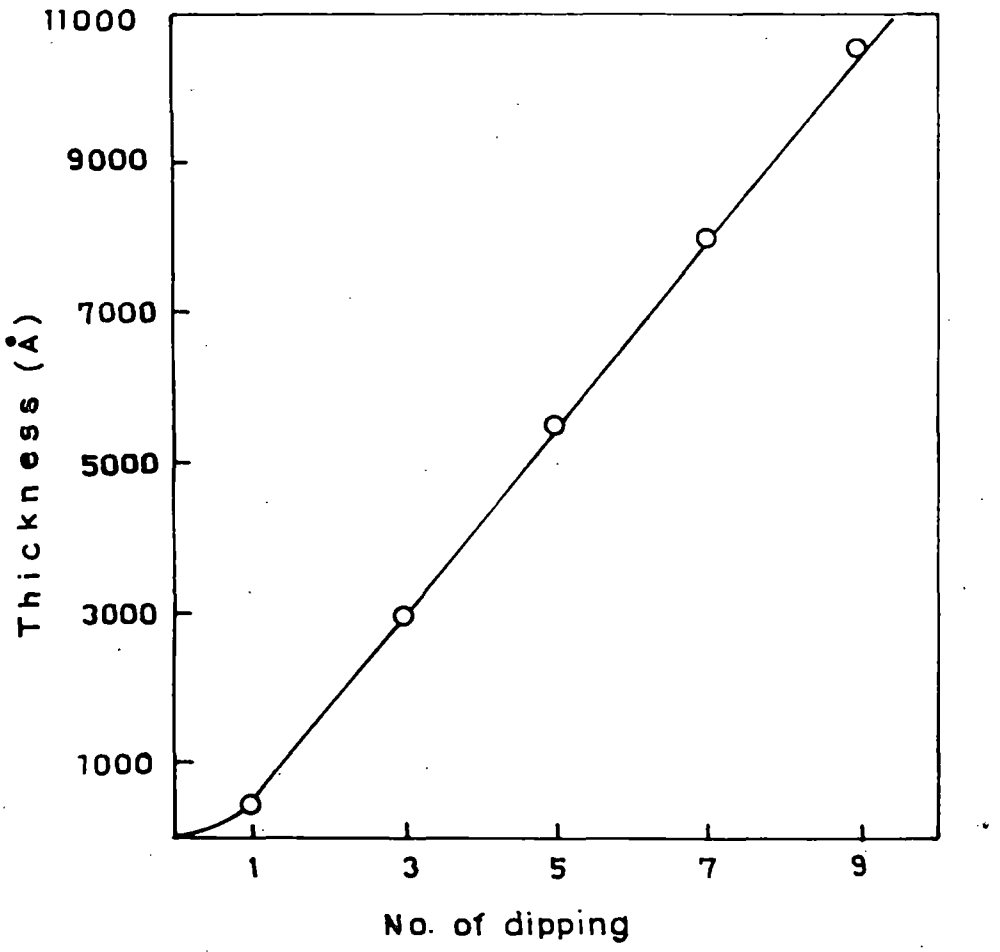

Figure 3.12. Dependence of thickness on number of dippings of SnS_2 thin films (speed = 1.33 mm/sec), $T_B = 360^o$ C).

that of SnS_2 films. But the thickness in case of SnS films is less than that for SnS_2 films for a particular dipping.

Characterization results reported in this chapter are for films prepared by 5 dippings corresponding to a thickness of 0.50 μm for SnS and 0.55 μm for SnS_2 films.

3.2.3.2. X-RAY DIFFRACTOMETRIC STUDY

Figure 4.13 shows the X-ray diffraction patterns for SnS thin films at three different baking temperatures (200° C, 300° C and 360° C) and 5 minutes baking time. Only one peak was observed at 31.95° which was found to be strongest for films prepared at a baking temperature of 300° C. The corresponding 'd' value was found to be 2.8 A°, which is identical to the (040) spacings of SnS.

The X-ray diffraction pattern for a typical SnS_2 thin films prepared at a baking temperature of 360° C, is shown in figure 3.14. It was observed from the XRD pattern that there is only one peak at $2\theta = 15°$. The 'd' value calculated from the 2θ value and was 5.9 A°, corresponding to spacing of (001) plane of SnS_2. Peak position and corresponding 'd' values of both SnS and SnS_2 films were compared with the standard JCPDS data file (No. 14-620 for SnS and No.23-677 for SnS_2), which confirmed the successful deposition of SnS and SnS_2 films. Prominent peaks and their corresponding d-values for SnS and SnS_2 films deposited on soda-glass substrate are listed and compared with d-values from JCPDS data file in table -3.1

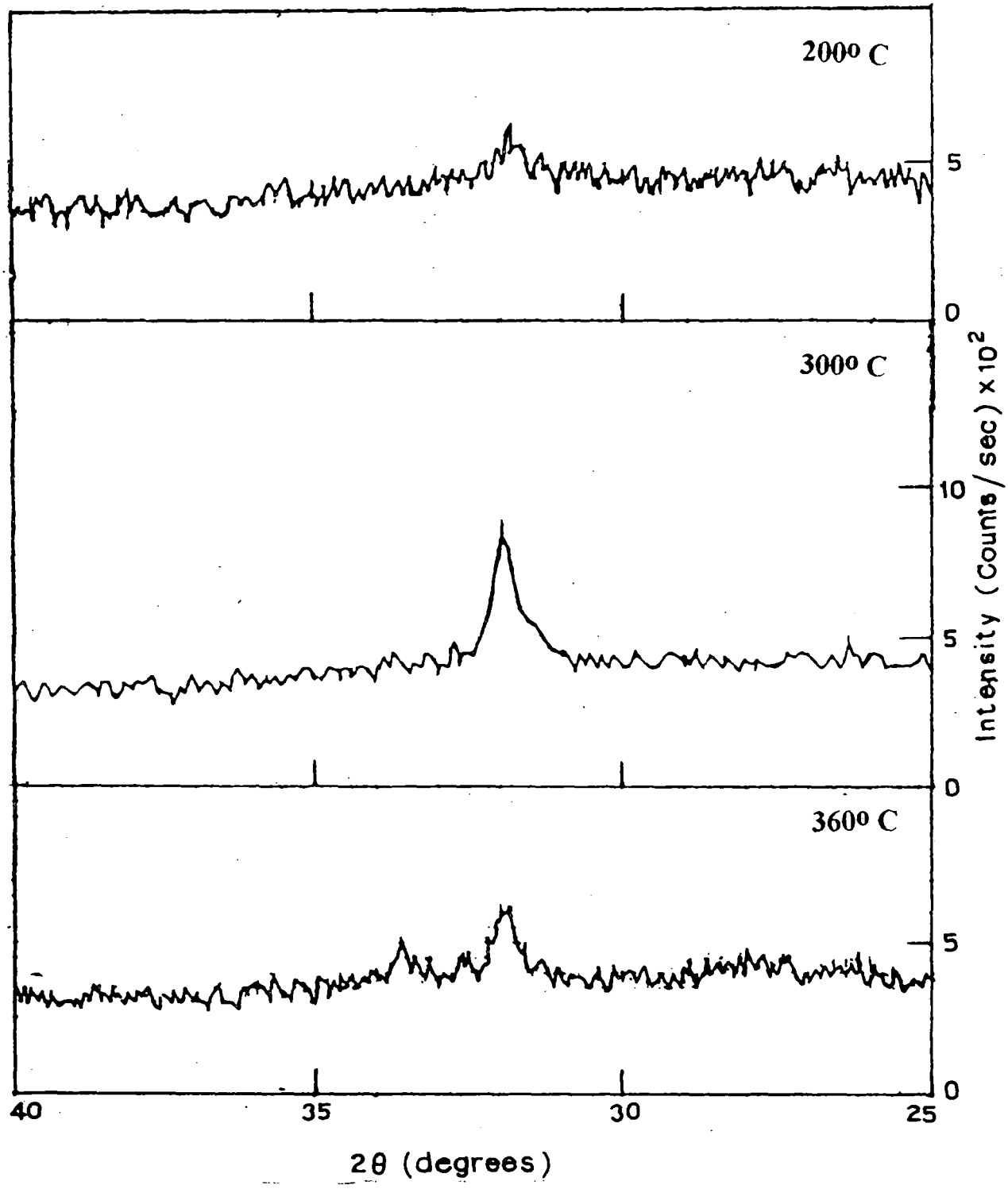

Figure 3.13. X-ray diffractograms of SnS thin films at various baking temperatures (T_B = 200° C, 300° C, 360° C).

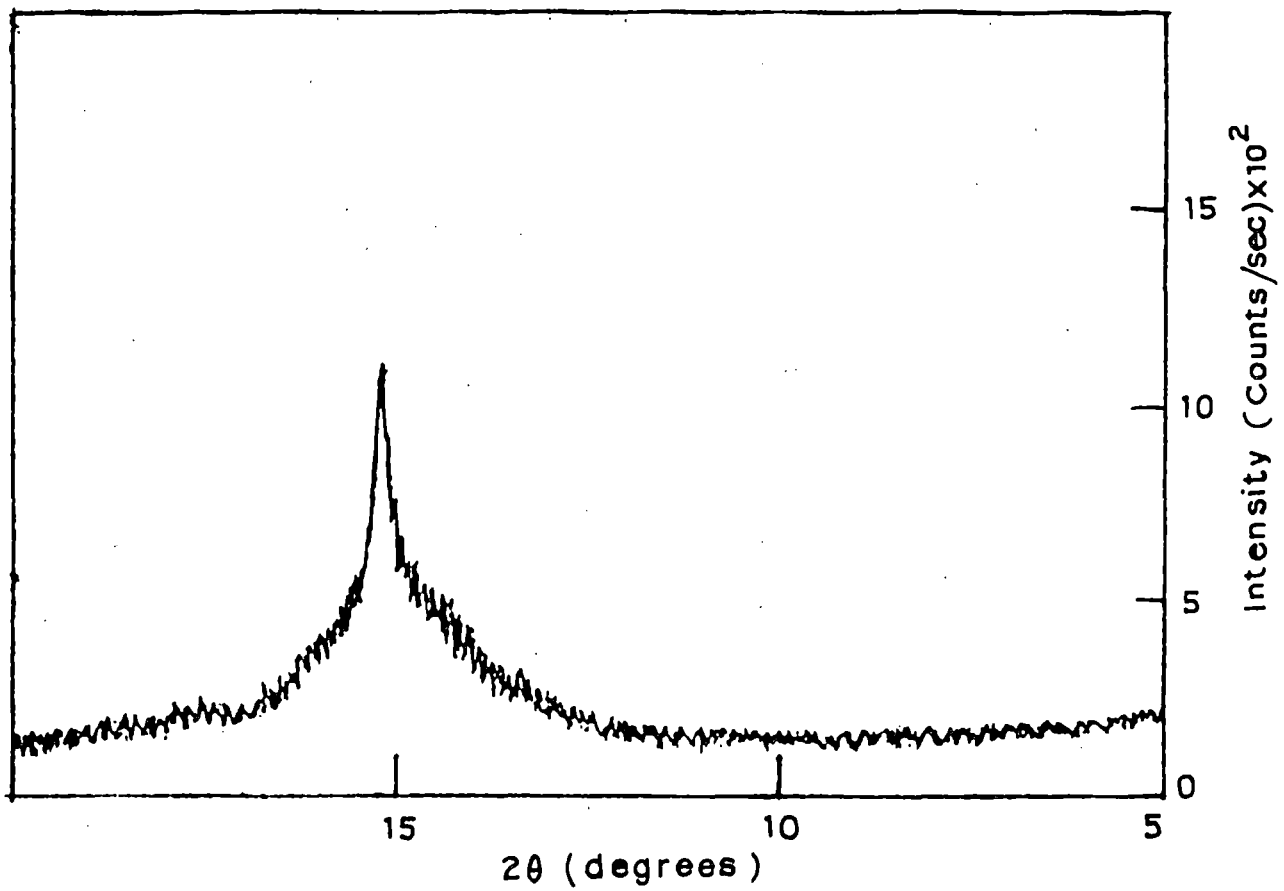

Figure 3.14. X-ray diffractograms of SnS_2 thin films (T_B = 360° C).

Table - 3.1. Prominent peak position (2θ values) of x-ray diffraction peaks,corresponding d-values and their identification for SnS and SnS_2 films deposited on glass substrate.

OBSERVATION			*COMPARISON WITH JCPDS FILE*			*hkl*
Peak position (2θ)	Observed d- values (A°)	Intensity (I/I_0)	Peak position (2θ)	Comparable d- values (A°)	Intensity (I/I_0)	
SnS Film ***(JCPDS data file No. 14-620)***						
31.95	2.80	100	32.00	2.79	100	040
SnS_2 Film (JCPDS data file ***No.23-677).***						
15.02	5.89	100	15.02	5.89	100	001

In each case, appearance of only one sharp peak appears to indicate a preferred orientation, along the (040) planes for SnS and (001) planes for SnS_2 respectively.

SnS_2 films prepared at 200° C and 300° C showed no sharp peaks and only a broad hump indicating that they were possibly amorphous.

Thus, baking for 5 minutes in 300° C and 360° C resulted in oxide-free SnS and SnS_2 films by the dip technique. It may be mentioned that no evidence of any oxide (SnO_2) peak was found over a 2 θ range 10° to 80°.

3.2.3.3. SURFACE MORPHOLOGY

SEM micrographs of SnS thin Films deposited at three different baking temperatures (200° C, 300° C and 360° C) are shown in figure 3.15. It is clear from the micrographs that grain size of the films deposited at 300° C is the largest compared to others. As already mentioned, these films also show the strongest XRD peaks.

Figure 3.16 shows the SEM micrographs of an SnS_2 thin film prepared at a baking temperature of 360° C. Average grain size for both SnS and SnS_2 films as observed from the micrograph is about 1 μm.

3.2.3.4. PHOTOCONDUCTIVE PROPERTIES

The spectral response of photoconductivity curves for SnS and SnS_2 thin films are shown in figure 3.17. In figure 3.17 the photocurrent values are normalised with the peak response for SnS_2 film taken as 1. The maximum photocurrent for SnS film is seen to occur at 840 nm, corresponding to a band gap of 1.4 eV which is comparable to values reported in the literature [39]. In case of SnS_2 films, the maximum photocurrent was observed at 500 nm which corresponds to a band gap of 2.4 eV, and compares quite well with values reported by other workers [39-40].

3.2.3.5. OPTICAL ABSORPTION PROPERTIES

In the following, the optical absorption of undoped and Sb-doped SnS_2 films are discussed. It was not possible to carry out optical absorption measurements on SnS films as the absorption edge lies in the infrared and the soda-glass substrate strongly absorbs in this range.

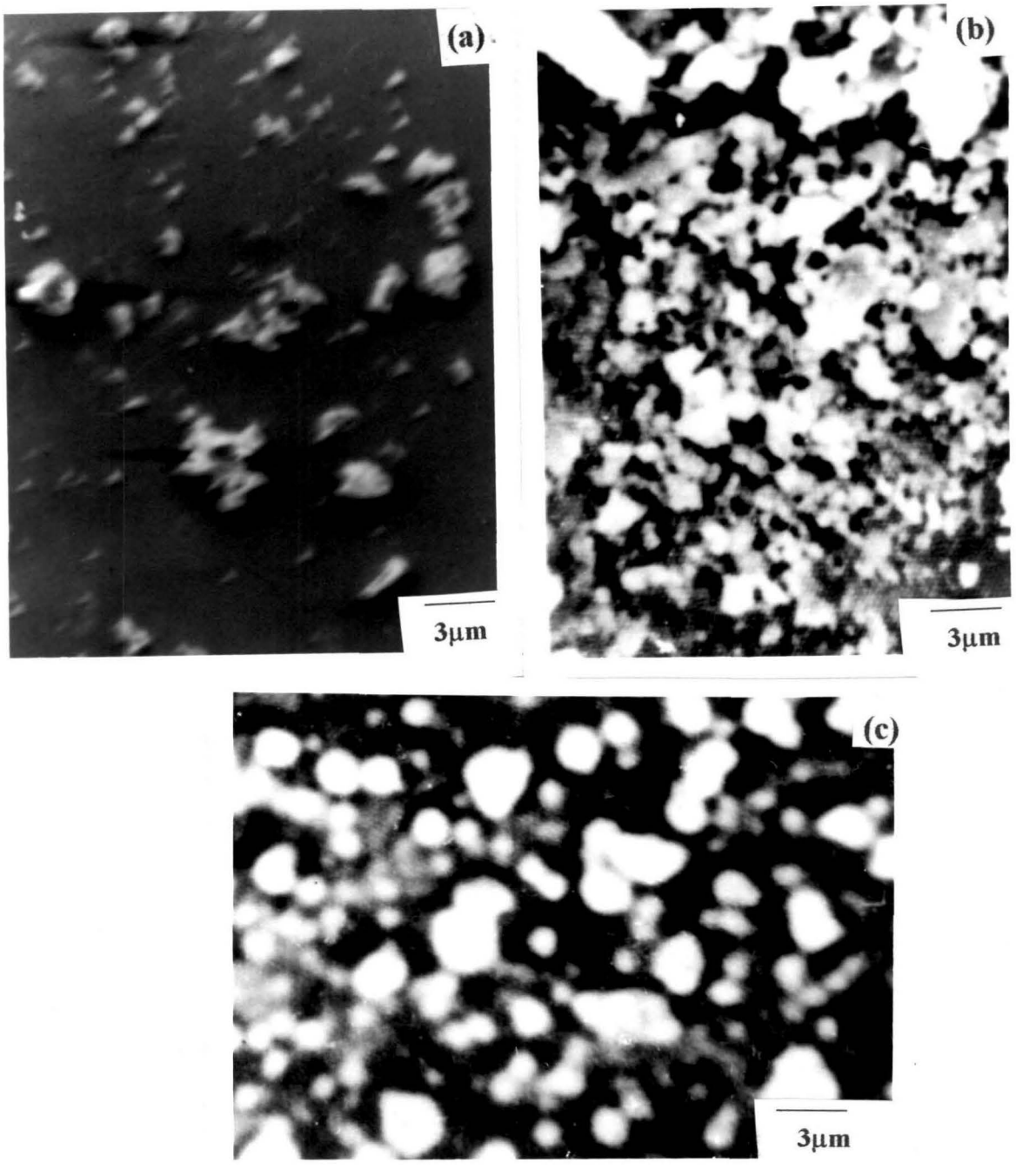

Figure 3.15. Scanning electron micrographs of SnS thin films at three different baking temperatures, (a) 200° C, (b) 300° C, (c) 360° C.

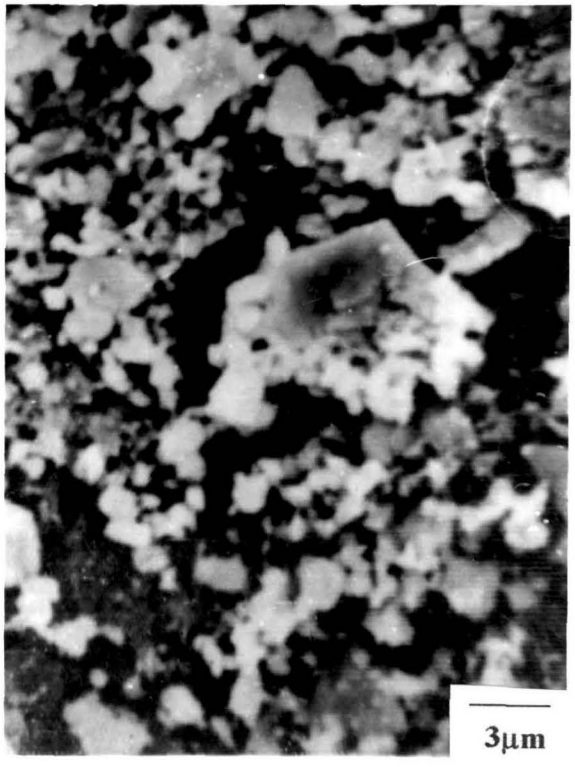

Figure 3.16. Scanning electron micrograph of SnS_2 thin films deposited on glass substrate at 360° C.

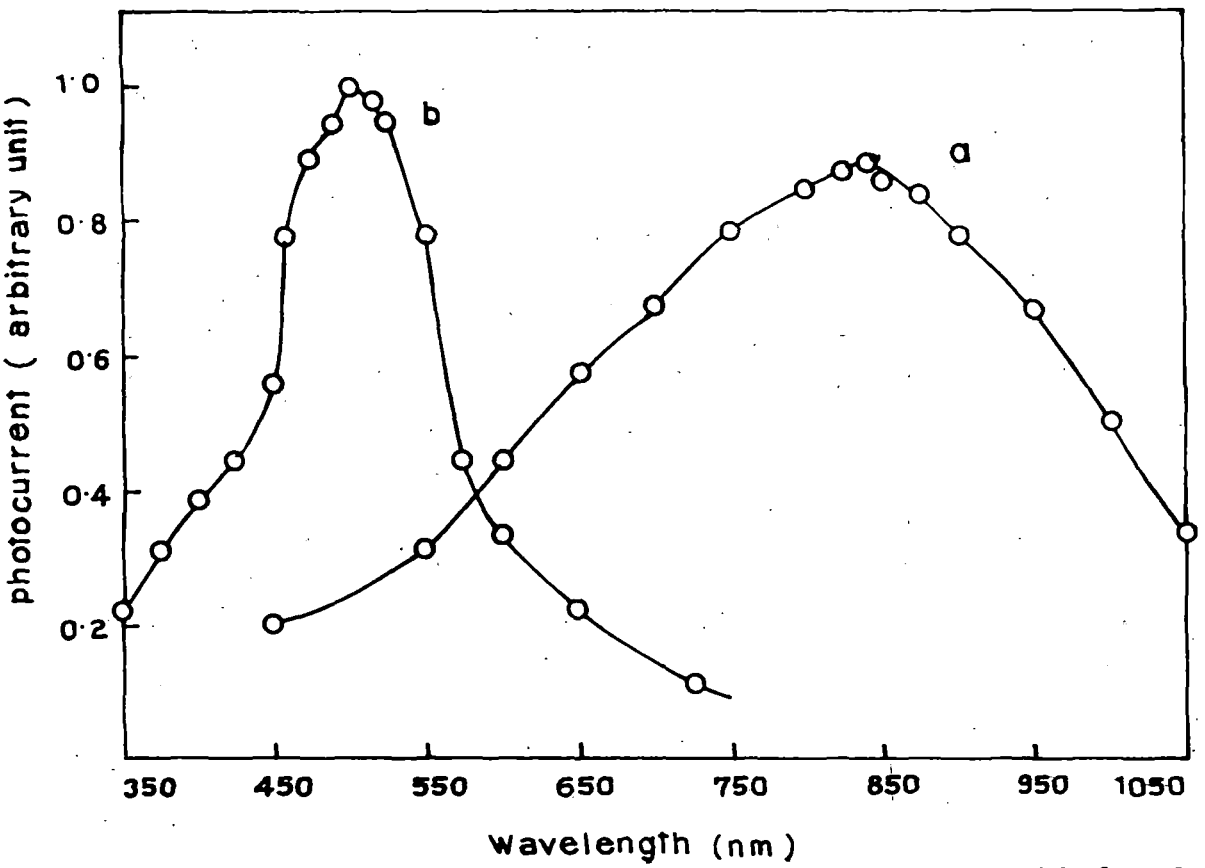

Figure 3.17. Spectral response of photoconductivity curves of SnS and SnS_2 thin films at baking temperature 300° C and 360° C respectively (a) SnS thin film and (b) SnS_2 thin film.

3.2.3.5.1. Undoped SnS_2 films

Optical absorption spectra of SnS_2 films is shown in figure 3.18. In this figure (a) shows the absorption spectra of pure SnS_2 film. The spectra is taken with respect to the bare substrate placed in the reference beam. The rise in absorption is quite steep, indicating that the films are homogeneous and the optical band gap was measured from the extrapolation of the linear portion of the $(\alpha h\nu)^2$ versus $h\nu$ curve shown in figure 3.19. The optical band gap of SnS_2 films is 2.4 eV (from figure 3.19), which is the same as obtained from photoconductive response data.

3.2.3.5.2. Sb-doped SnS_2 films

SnS_2 thin films of thickness about 0.55 μm deposited at a baking temperature of 360° C for 5 minuits baking time were doped with antimony (Sb) for different at%. It was observed from the optical absorption data in figure 3.18, that the absorption edges of these spectra are shifted towards shorter wavelength as a result of increasing Sb concentration corresponding to an increase in band gap from 2.4 eV to 3.0 eV (for 3 at%doping), which was calculated from the curve $(\alpha h\nu)^2$ versus $h\nu$ shown in figure 3.19.

X-ray diffractometric studies were carried out for doped SnS_2 films. It is observed that introduction of antimony (Sb) as a dopant in the SnS_2 film reduces the peak height. In the X-ray diffractogram shown in figure 3.20, thus at 0.12 at% Sb doped SnS_2 film the peak height is reduced and for 0.3 at% Sb doping the peak has disappeared. Thus it can be concluded that Sb-doping has a strong effect on the crystallinity of SnS_2, and a very small concentration (0.3 at%) of Sb being sufficient to make it completely amorphous. A similar result was observed by Banerjee et al. [51], who found that the introduction of Sb as dopant in CdS reduces its crystallinity and, at 3 at% doping, the structure becomes completely amorphous.

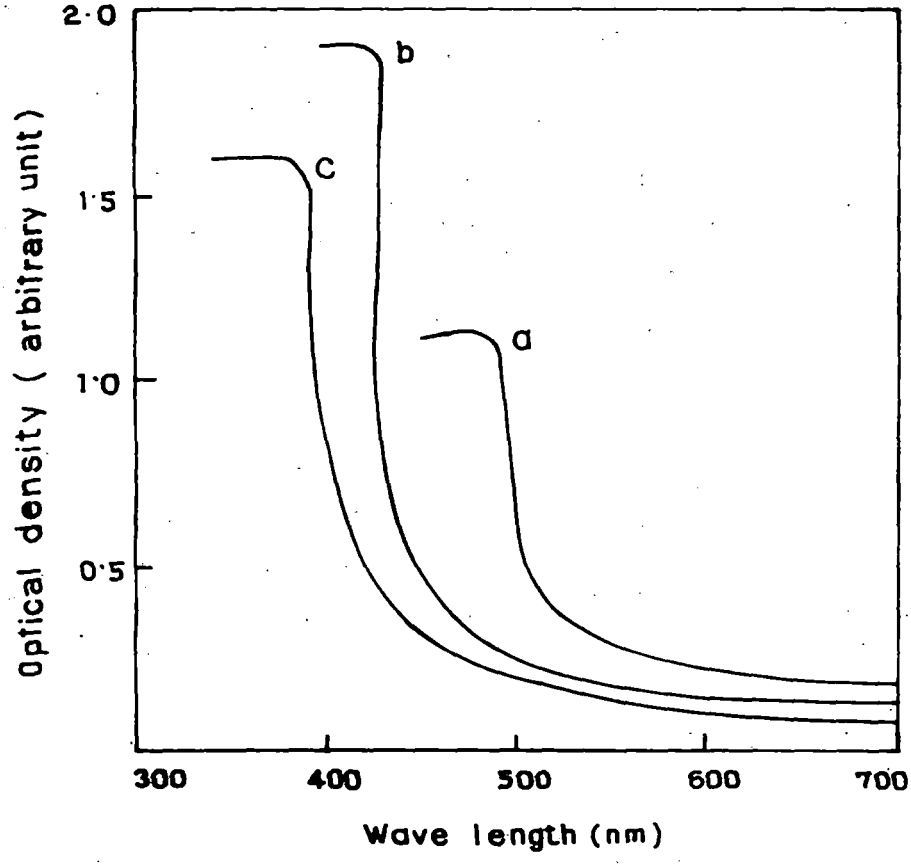

Figure 3.18. Optical absorption spectra of undoped SnS_2 and different at% dopped SnS_2 thin films at baking temperature 360° C ;(a) undopped SnS_2 , (b) 0.12 at% Sb dopped SnS_2 and (c) 0.32 at% sb dopped SnS_2 thin films.

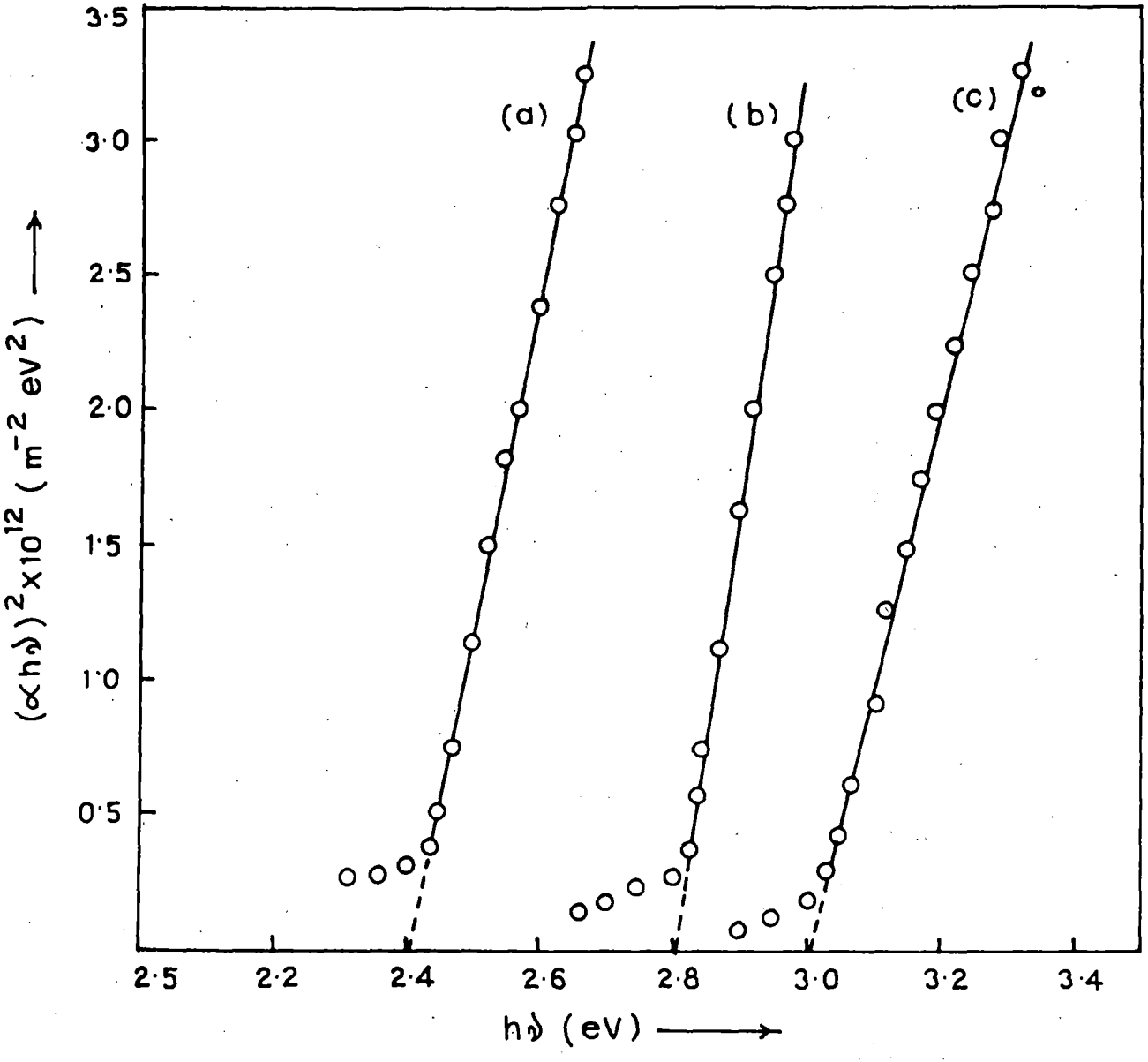

Figure 3.19. Plots of $(\alpha h\nu)^2$ against hν curves of undoped and Sb-doped SnS_2 thin films. (a) Undoped SnS_2 films; (b) SnS_2:Sb 0.12 at%; (c) SnS_2:Sb 0.32 at%.

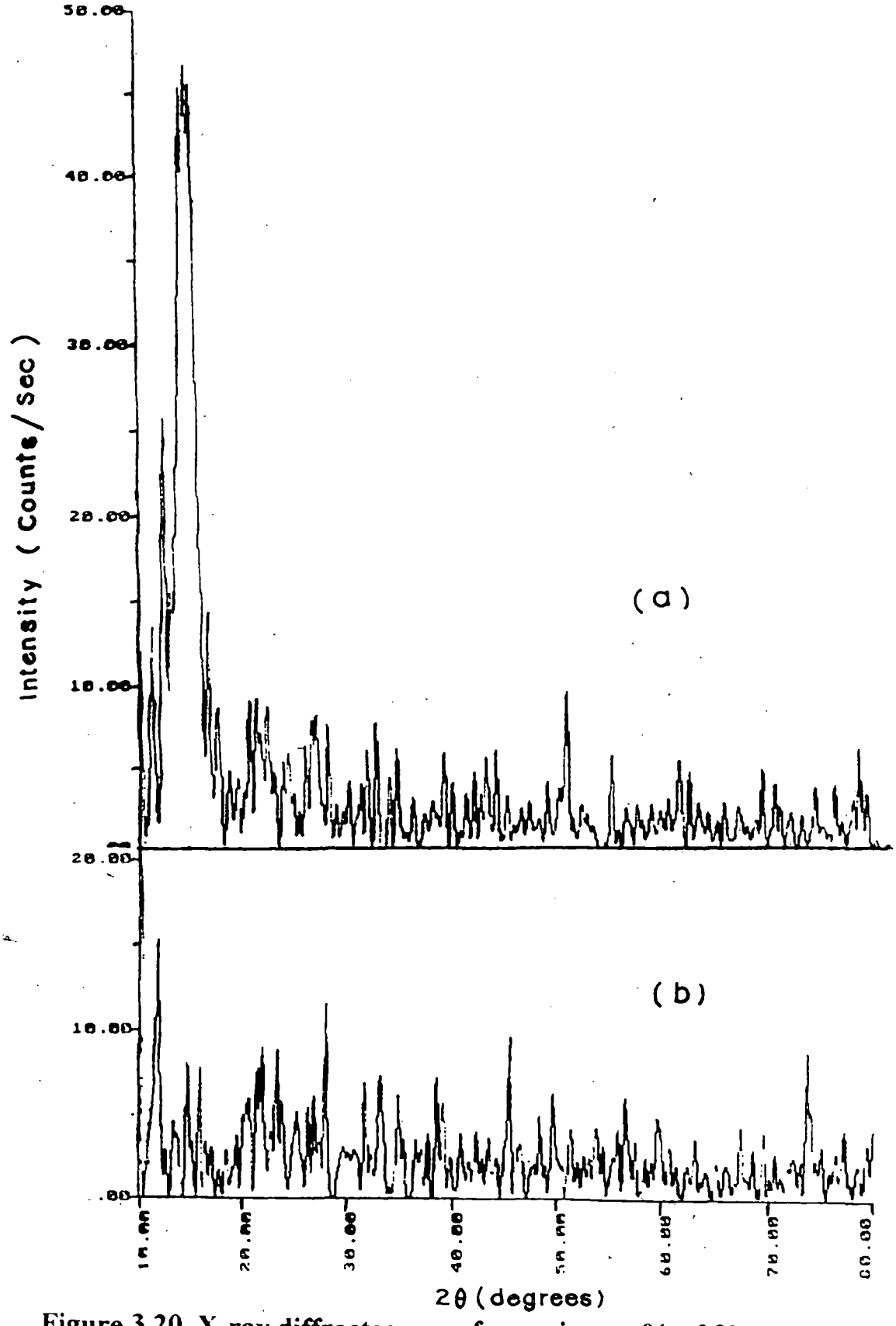

Figure 3.20. X-ray diffractograms for various at% of Sb dopped SnS_2 thin films at baking temperature 360° C (a) 0.12 at% and (b) 0.3 at%.

3.2.3.6. EFFECT OF ANNEALING

Effect of annealing was studied by baking SnS and SnS_2 films, prepared at a baking temperature of 300° C and 360° C for 5 minutes to a higher temperature of 400° C in the furnace at atmospheric condition for various baking times.

We found that when SnS and SnS_2 films are annealed in a furnace at 400° C for more than 10 minutes, these are converted into SnO_2 transparent conducting films in the presence of atmospheric oxygen, according to one of the following reactions.

$$SnS + 2O_2 = SnO_2 + SO_2 \text{ ---------(3.9)}$$

$$SnS_2 + 3O_2 = SnO_2 + 2SO_2 \text{ -------(3.10)}$$

Figure 3.21 shows the effect of annealing in atmospheric condition at 400° C for different baking times on the sheet resistance of SnS and SnS_2 films. It was observed that good quality SnO_2 films in terms of crystallinity as well as optical transmission could be obtained by air annealing of tin disulphide films prepared by dip technique for about 50 minutes. The electrical conductivity SnO_2 films obtained by this method are quite reasonable, the sheet resistance being 2 X 10^3 Ω/□ with an optical transmission of 90%.

It was observed that for prolonged annealing (>120 min.) of SnS and SnS_2 films the sheet resistance become very high and of the order of 10^6 Ω/□ with no change in optical transmission.This is probably due to the filling of the oxygen vacancies resulting in a near-stoichiometric materials. These high-sheet-resistance SnO_2 films may be useful as an insulator layer [52] as well as a protective layer [48] in semiconductor device structures. It was observed that due to increase in annealing time the optical transmission of the films is increase (fig. 3.22). XRD and SEM of a typical SnO_2 films obtained by this method by annealing of SnS_2 is shown in figures 3.23 and 3.24. The XRD pattern of the

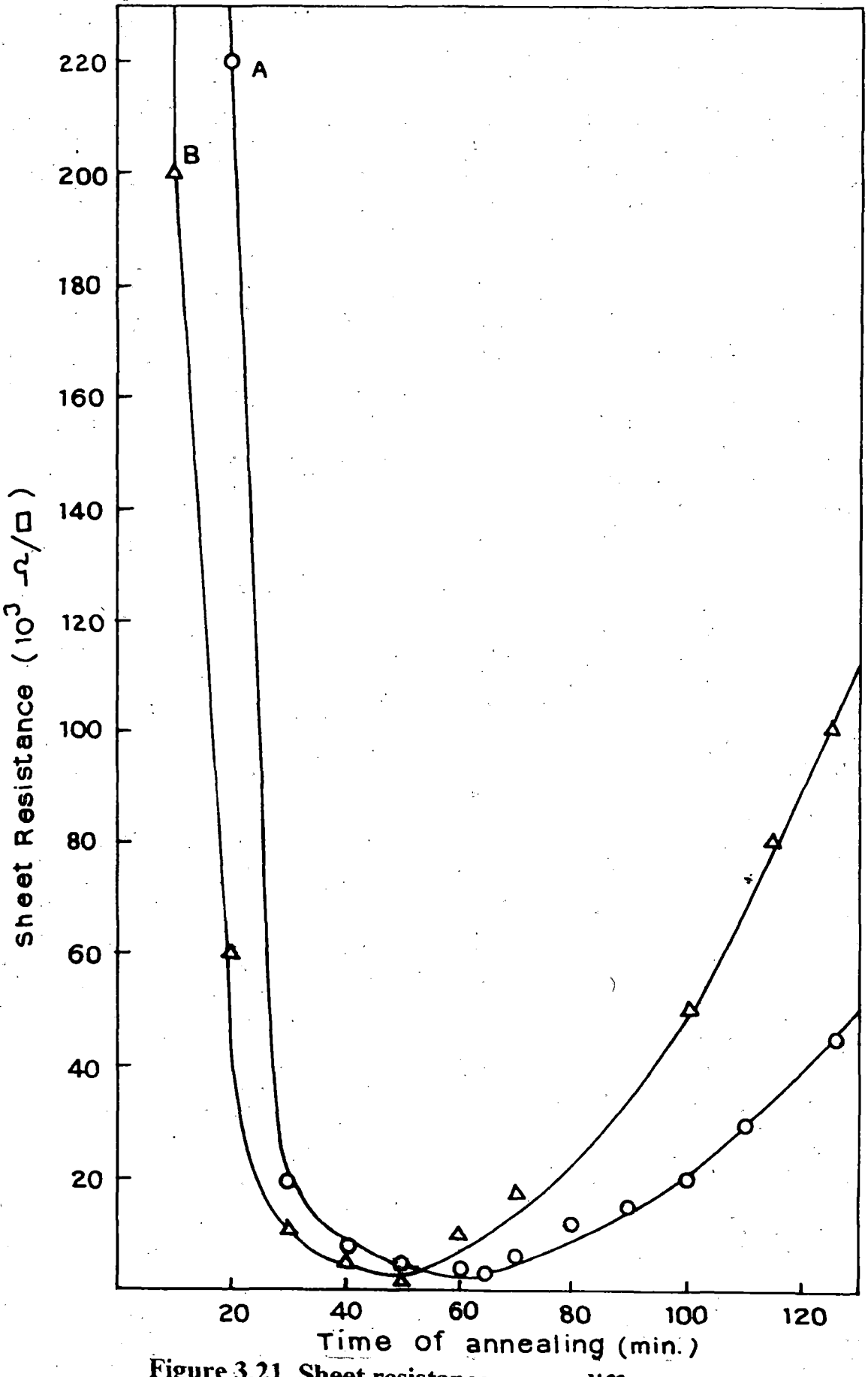

Figure 3.21. Sheet resistance versus different baking time of annealing of A, SnS; B, SnS_2 films at 400° C.

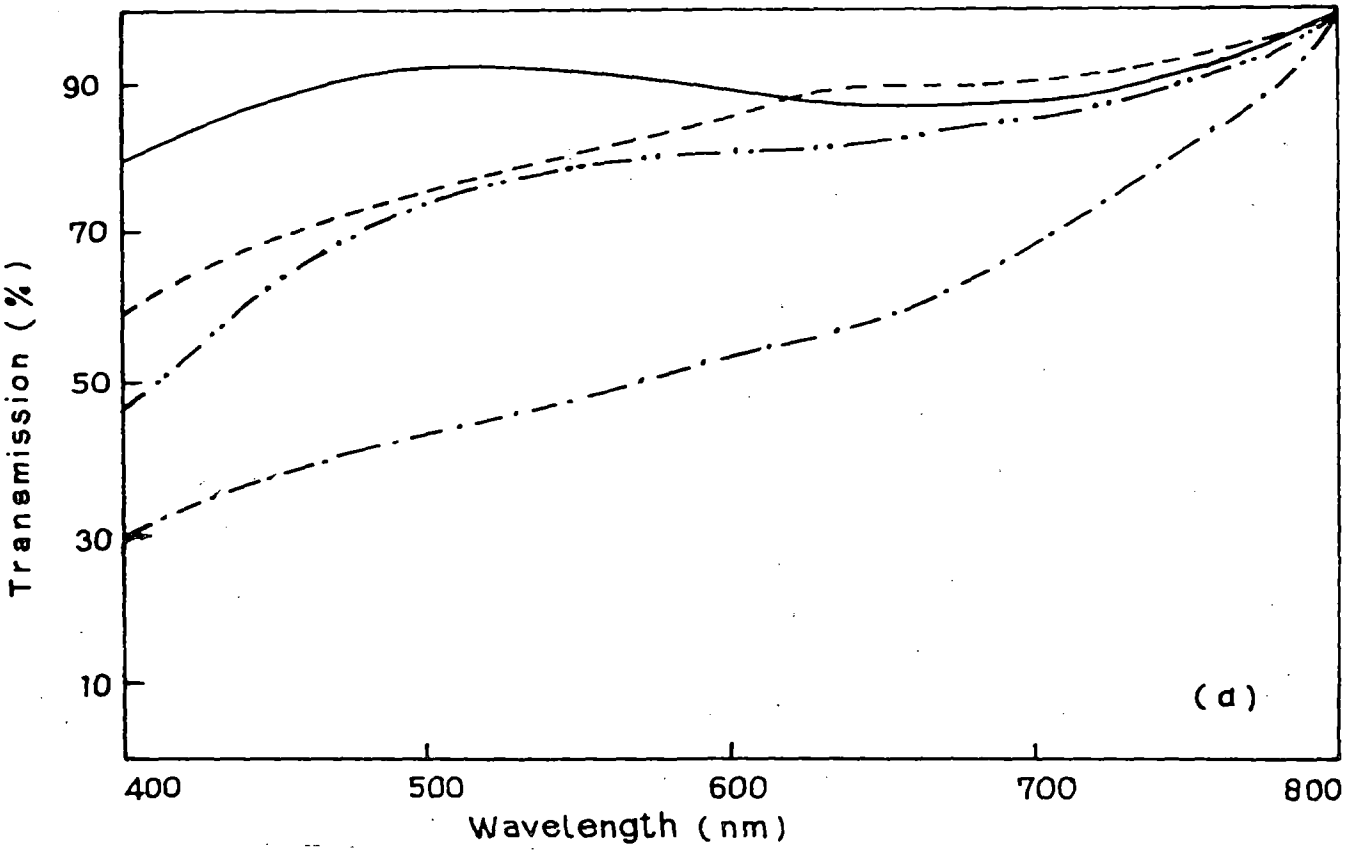

Figure 3.22. Optical transmission versus wavelength for annealed SnS thin films of various annealing /baking time(T_B).
(a) Annealed SnS thin film: (-.-.-.-.), T_B =30min.; (-..-..-..-..), T_B=60 min.; (———), 75 min.; (_____), T_B=90 min.

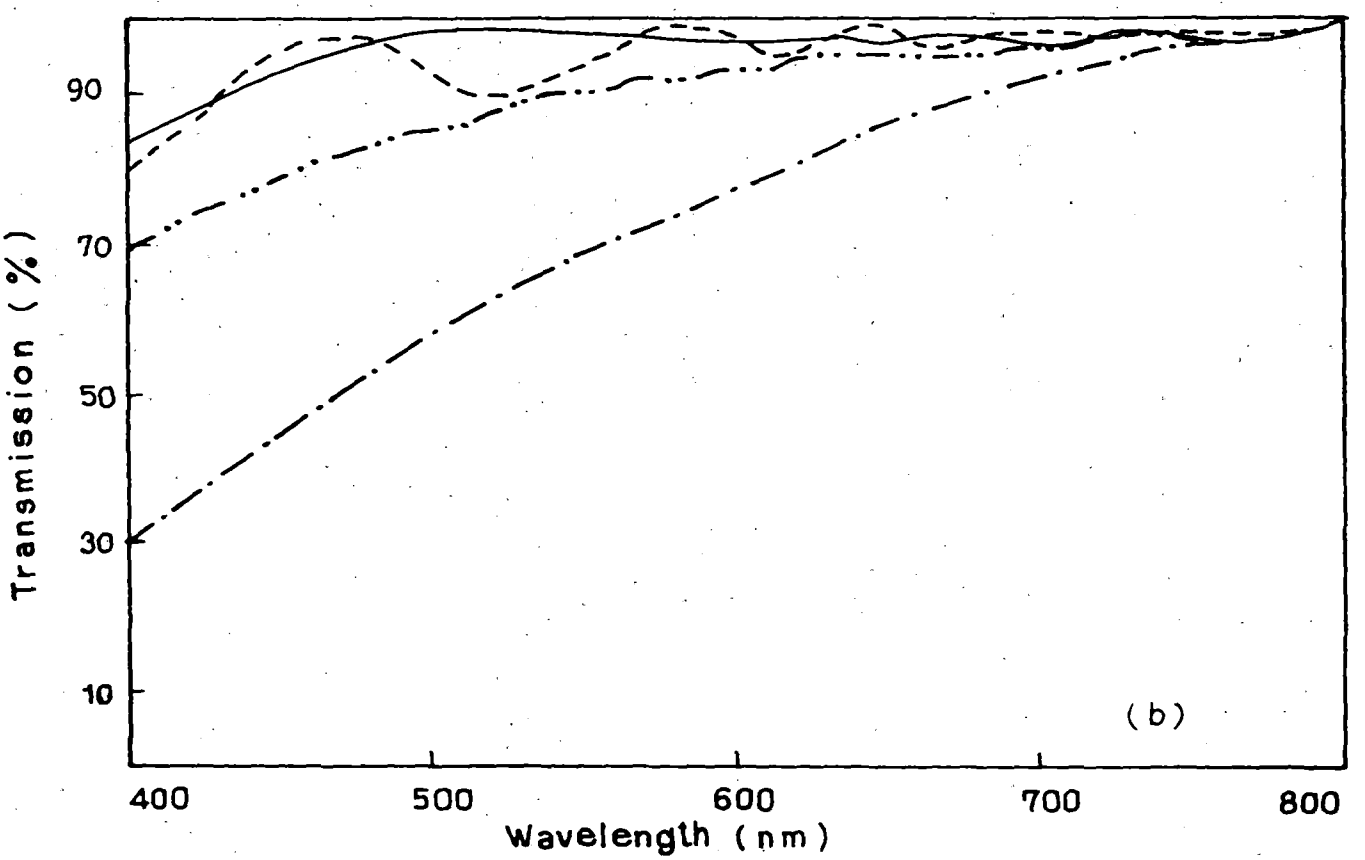

Figure 3.22. Optical transmission versus wavelength for annealed SnS_2 thin films of various annealing /baking time(TB).
(b) Annealed SnS_2 thin film: (-.-.-.-.), T_B =30min.; (-..-..-..- ..), T_B=50 min.; (———),T_B=75 min.; (_____),T_B=90 min.

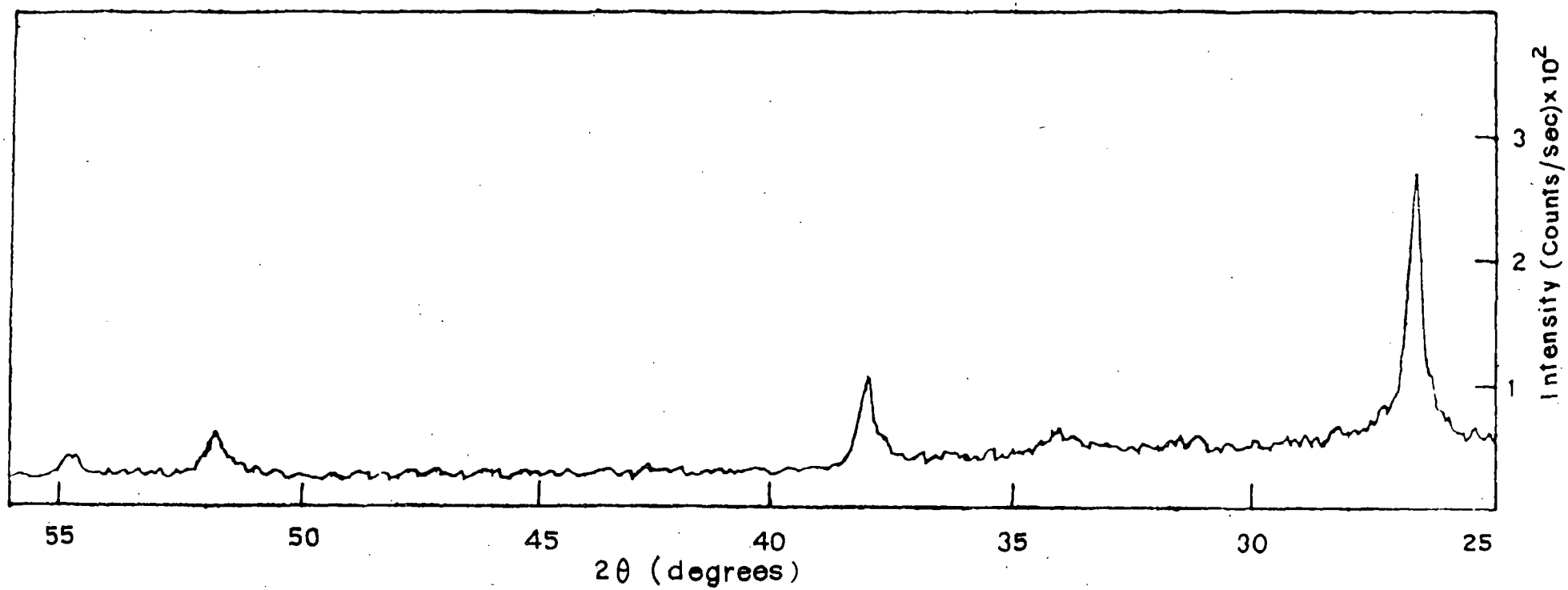

Figure 3.23. X-ray diffractograms for SnO_2 film obtained from SnS_2 film by atmospheric annealing at 400° C.

transformed films matches well with the XRD powder pattern simulated from the data for SnO_2 [53] as well as with JCPDS file 21-1250 data for SnO_2 mineral sample. Prominent peaks, corresponding d-values and their intensity for these SnO_2 films are listed and compared with JCPDS data file in table -3.2

Table - 3.2. Prominent peak position (2θ values) of x-ray diffraction peaks, corresponding d-values and their identification for SnO_2 film obtained from SnS_2 film (annealing time = 50 minutes).

OBSERVATION			*COMPARISON WITH JCPDS DATA FILE NO. 21-1250*		*hkl*
Peak position (2θ)	Observed d- values (A°)	Intensity (I/I_o)	Comparable d- values (A°)	Intensity (I/I_o)	
26.65	3.34	100	3.35	100	110
38.00	2.36	40	2.37	25	200
51.85	1.76	22	1.76	65	211
54.80	1.67	15	1.67	18	220

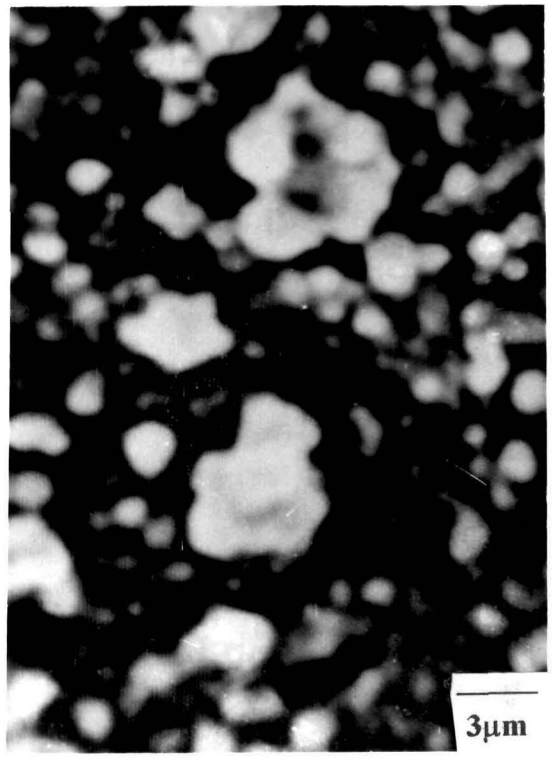

Figure 3.24. Scanning electron micrograph of SnO_2 thin film obtained from SnS_2 film by atmospheric annealing at 400° C.

3.3. A FEW MORE SULPHIDE FILMS

A few more sulphide films were also deposited using dip technique. In the following section deposition and characterisation of Mo-sulphide and Cu-sulphide films have been discussed in brief.

*3.3.1. MOLYBDENUM DISULPHIDE (MoS_2) THIN FILM

3.3.1.1. INTRODUCTION

Molybdenum dichalcogenides appear to be very promising semiconductor materials for various applications such as solar cells [54-55], rechargeable batteries [56] and solid lubricants for metallic and ceramic surface in environments where hydrocarbon or other fluid-based lubricants are unsuitable, such as in high vacuum or high temperature applications [57-58]. It has been also widely used in space-technology where its low co-efficient of friction in vacuum is of particular value [59]. These applications arise from the optical, electrochemical and mechanical properties of these compounds. They exhibit a layer-type structure in which monolayers of Mo are sandwiched between monolayers of sulphur, which are held together by relatively weak van der Waals forces. These materials have band gaps (1.78 eV) well-matched to the solar spectrum [60]. A number of methods exist for the production of MoS_2 thin films, including sputtering [61-63], electrochemical deposition [60,64], and pulsed laser deposition [65-68].

In this section, the preparation of MoS_2 thin films by dip technique and to study their structural and optical properties have been described.

***Presented at the "Fifth West Bengal State Sc. Cong." Proceedings, University of North Bengal, 21-23 March, 1998, Page 140.**

3.3.1.2. EXPERIMENTAL DETAILS

Film deposition procedure exactly follows the same technique as discussed earlier, where lifting speed were 1.33 mm/sec and the starting solution was taken by mixing of methanolic solution of ammonium molybdate (5 gms ammonium molybdate in 50 cc methanol) and ammonium thiocyanate (3.88 gm ammonium thiocyanate in 40 cc methanol). The deposition was performed on soda-glass substrate at different baking temperature from 300° C to 450° C for 5 minutes baking time. The substrate was cleaned as discussed before in detergent solution, water and chromic acid and finally degreased in acetone and methanol vapour.

Characterization of the films were carried out by X-ray diffractometry, Scanning electron microscopy and optical absorption using PHILIPS diffractometer (model PW 1390) with CuK_{α} radiation (Ni-filter) at 1.54 Å, HITACHI S-530 scanning electron microscope and SHIMADZU UV-240 double-beam spectrophotometer respectively.

3.3.1.3. RESULTS AND DISCUSSION

MoS_2 thin films are smooth, uniform and strongly adherent to the substrate. The films are gray in colour. The thickness of the films prepared for characterization is estimated to be one micrometer.

Figure 3.25 shows the XRD spectra of MoS_2 thin films prepared at three different baking temperature 300° C, 360° C and 450° C. From the XRD spectra we observed that the films prepared at 300° C is completely amorphous in nature but films prepared at 360° C and 450° C are crystalline. Comparison of the prominent peak positions (2θ - values) of the XRD spectra with the ASTM data file for MoS_2 (File No. 24-515) suggests that the films deposited at baking temperature 360° C and 450° C are

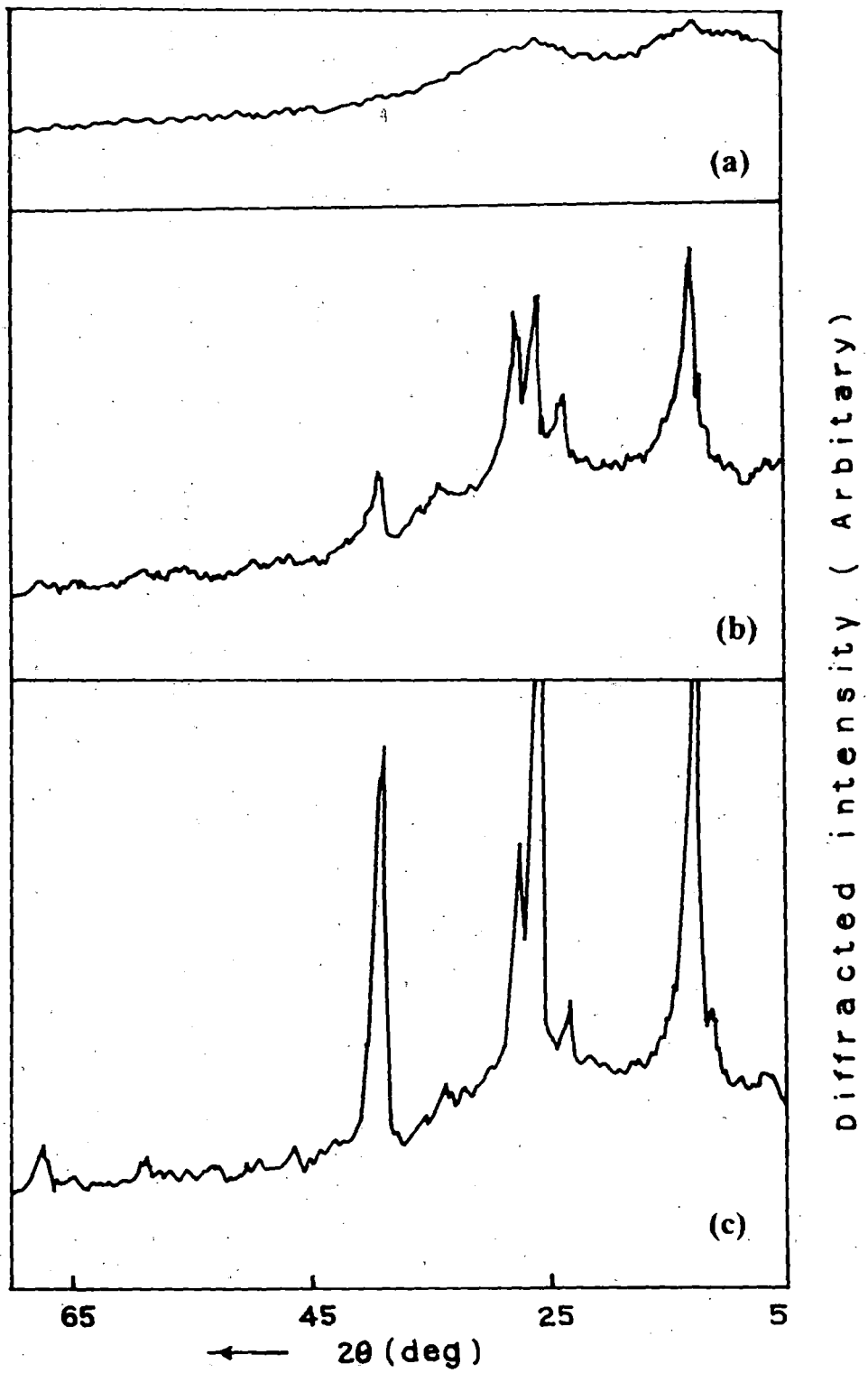

Figure 3.25. X-ray diffractogram of MoS_2 thin films deposited on glass substrate at three different baking temperature [(a), 300° C; (b), 360° C; (c), 450° C].

hexagonal in structure. The planes of MoS_2 are indicated in the XRD spectra. These planes are (002), (012), (104), (107) and (113). The peaks which are unmarked do not correspond to MoS_2 films. These unmarked peaks correspond to MoO_3 which were confirmed from the ASTM data file no. 5-0508. Prominent peaks, corresponding d-values and their intensities for MoS_2 films prepared at 450° C are listed and compared with JCPDS data file (24-515) in table -3.3

Table - 3.3. Prominent peak position (2θ values) of x-ray diffraction peaks, corresponding d-values and their identification for MoS_2 films.

OBSERVATION			*COMPARISON WITH JCPDS DATA FILE NO. 24-515*		*hkl*
Peak position (2θ)	Observed d- values (A°)	Intensity (I/I_0)	Comparable d- values (A°)	Intensity (I/I_0)	
13.25	6.30	100	6.20	100	002
33.75	2.65	33	2.63	21	012
39.00	2.30	88	2.35	27	104
46.40	1.95	28	1.90	14	107
59.00	1.56	25	1.53	8	113

Figure 3.26 shows the scanning electron micrographs of MoS_2 films deposited on glass substrates at three different baking temperatures. These micrographs shows that the grain size of MoS_2 films when deposited at 360° C and 400° C are larger than the that size of films deposited at 300° C.

Figure 3.27 shows the optical absoption of MoS_2 films deposited on glass substrate. From the steepness of the absorption edge we conclude that the films are homogeneous. The optical bandgap is calculated from the plot of $(\alpha h\nu)^2$ versus $h\nu$ (Fig. 3.28) and is found to be 1.80 eV. This is comparable with the value 1.78 eV obtained by Ponomarev et al.[60].

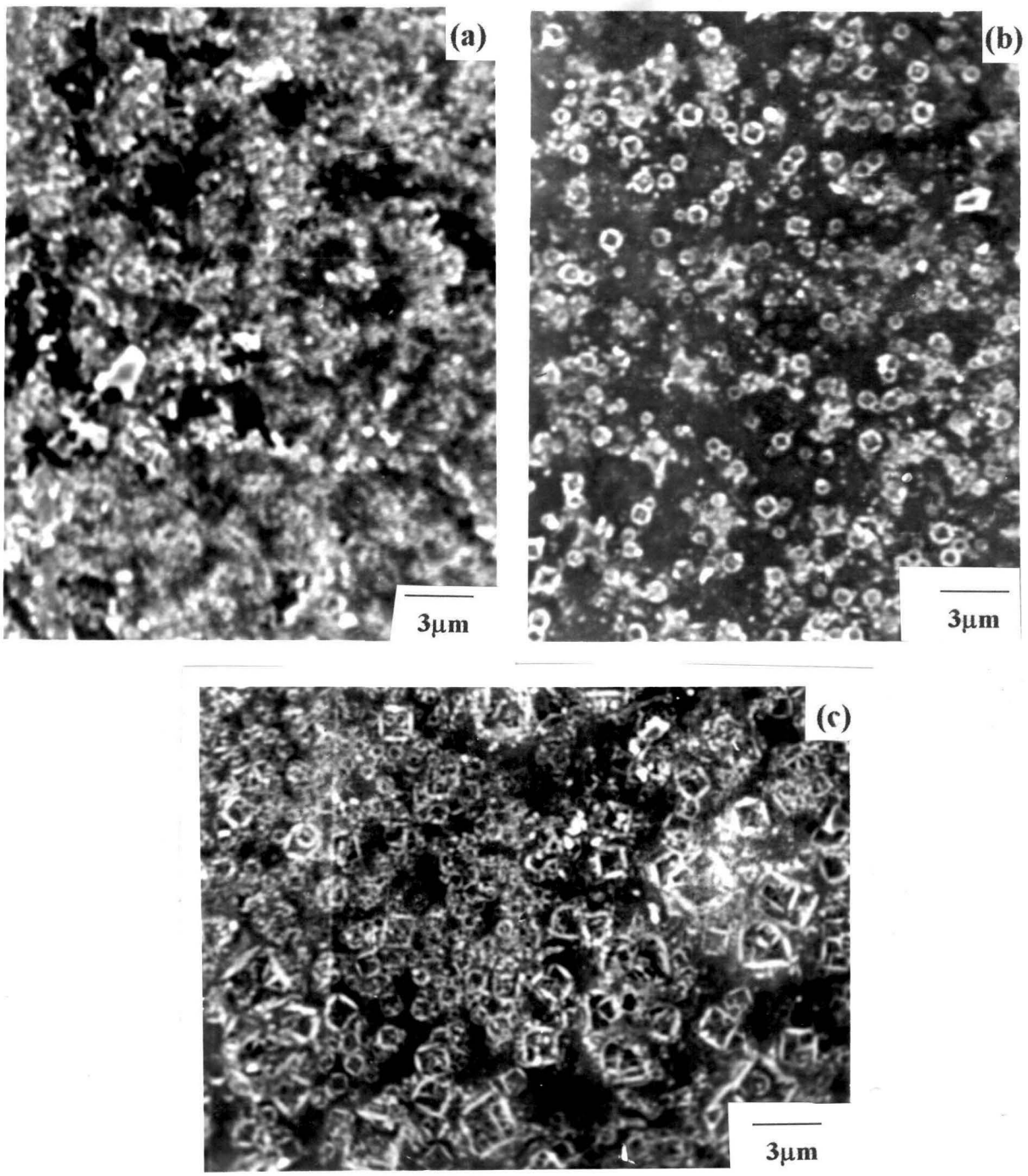

Figure 3.26. Scanning electron micrograph of MoS_2 thin film obtained from deposited on glass substrate at three different baking temperatures [(a), 300° C, (b) 360° C, (c) 450° C.]

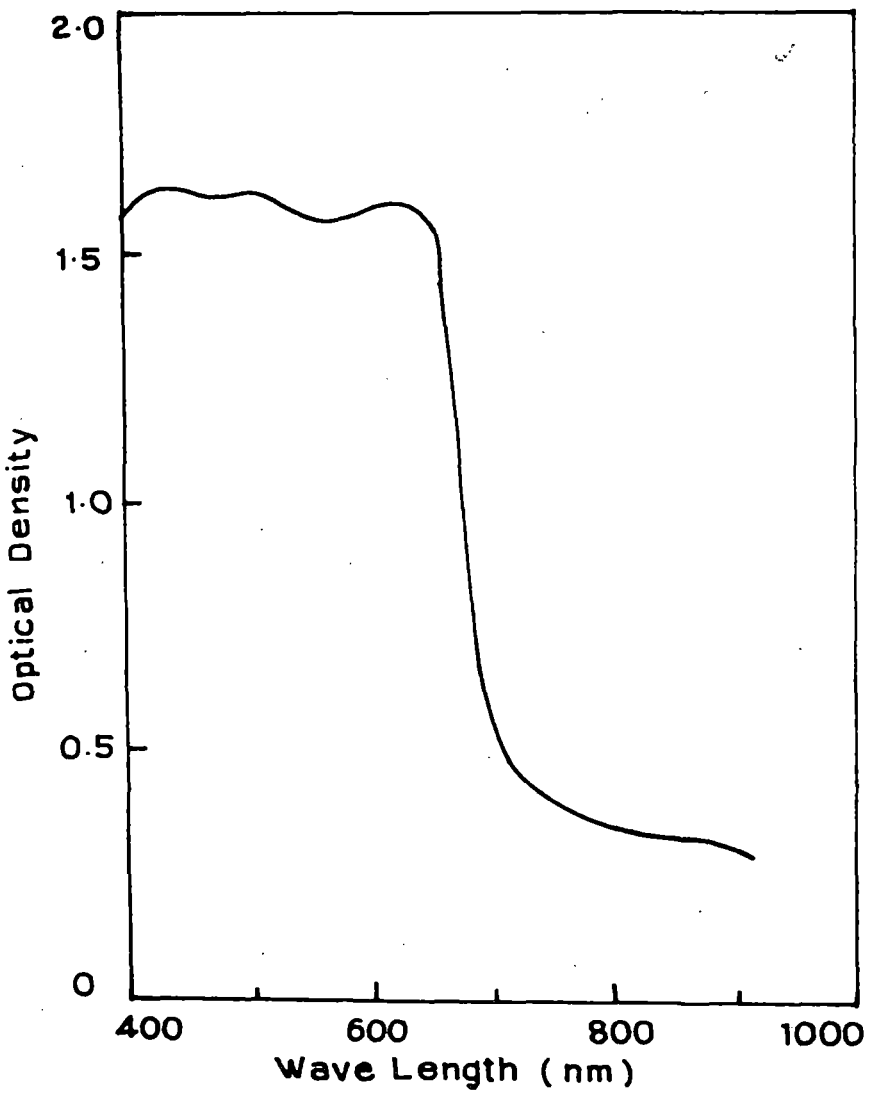

Figure 3.27. Optical absorption spectra of MoS_2 thin films deposited on glass substrate.

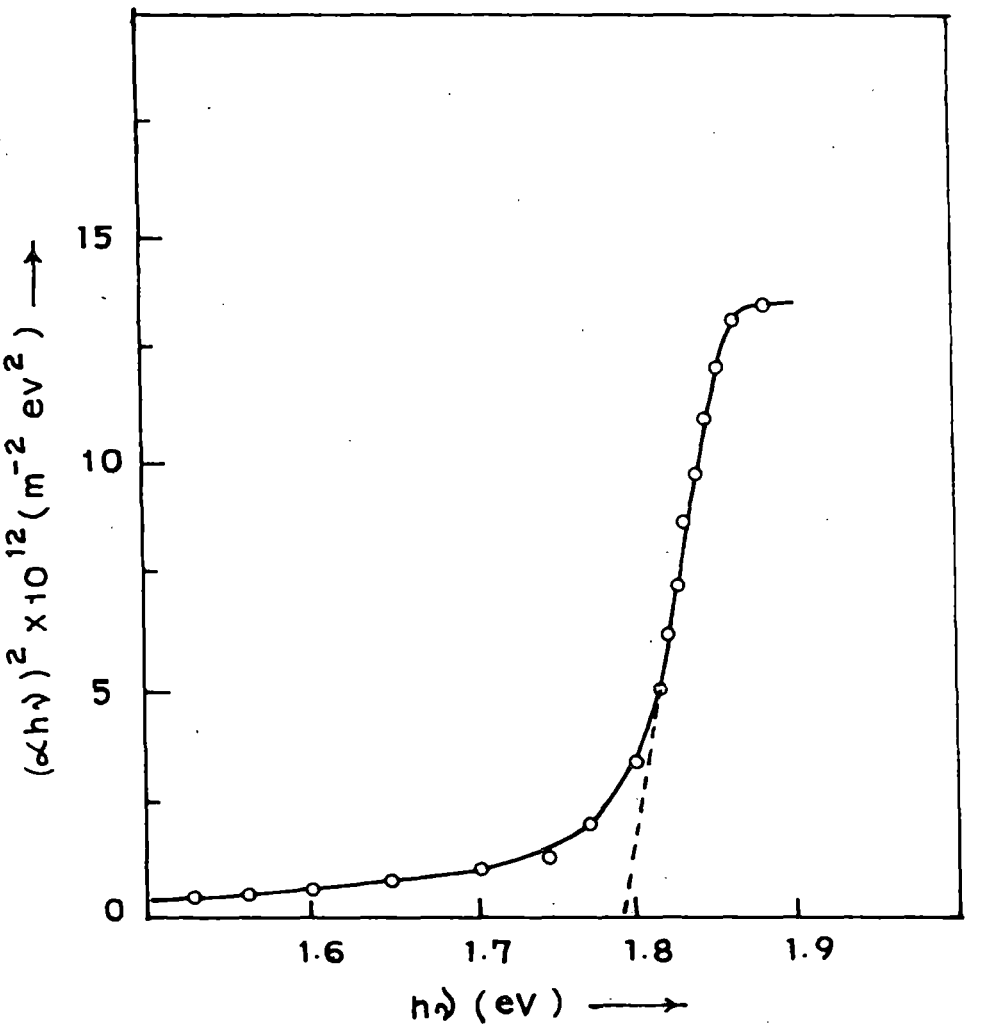

Figure 3.28. Plots of $(\alpha h\nu)^2$ against hν curves of MoS_2 thin films.

3.3.2. COPPER SULPHIDE (Cu_2S) THIN FILM

3.3.2.1. INTRODUCTION

The copper-sulphide Cu_xS ($1 \leq x \leq 2$) system forms a number of phases, which are well known for their application as optoelectronic materials, and continue to be interesting semiconductor materials due to the variation in properties depending on the value of x [69-72]. At least four stable phases are known [73] to exist at room temperature for which their mineralogical names are often used. On the 'copper rich' side of the copper sulphide phase diagram are the orthohorhombic chalcocite (Cu_2S), djurlite ($Cu_{1.95}S$) and anilite ($Cu_{1.75}S$), while in the 'sulphur rich' side is covellite (CuS). Mixed phases are also known in the intermediate composition [74]. The structure of the copper sulphide compounds is quite complicated [75]. Even the structures of Cu_2S and CuS, which appear to be stoichiometric, are not consistent with their formulation as Cu(I) and Cu(II) sulphides. Chalcocite (Cu_2S) can come in its low-temperature from with a rather complex structure or in its high-temperature from of disordered rearrangements of Cu atoms in a close-packed array of S atoms [76]. Likewise, the compound CuS, which occurs as the mineral covellite, has one -third of its metal ions surrounded by three neighbouring S atoms at the corners of a tringle and the remainder have four S neighbours arranged tetrahedrally.

Copper sulphides exhibit a range of electrical properties, from metallic to semi-metallic and semiconductor-like. Due to these characteristics, by suitably adjusting their composition copper sulphides are exploitable in the fabrication of electronic devices [76-77].

Deposition of these films can be made by different techniques, such as vacuum evaporation [78], activated reactive evaporation [79] and chemical bath deposition [80-84].

In this section, the preparation, structural and optical properties of dip deposited Cu_2S thin films have been described shortly.

3.3.2.2. EXPERIMENTAL DETAILS

Film preparation and other parameters was the same as discussed earlier, the only difference being the starting material and the baking temperature. For depositon of Cu_2S films, methanolic solution of copper nitrate (10 gms of copper nitrate in 40 cc methanol) and ammonium thiocyanate (1.6 gms ammonium thiocyanate in 20 cc methanol) were mixed together slowly to yield the starting solution. Films were deposited on soda-glass substrates at three different baking temperature 360° C, 400° C and 500° C for five minutes baking time. Multicoating (5 dip) films having thickness of about 1μm was taken for the characterization of the films. The colour of the films are brown.

For structural properties x-ray diffractometry and surface morphology studies were carried out by PHILIPS diffractometer (model PW 1390) with CuKα radiation (Ni-filter) at 1.54 A° and HITACHI S-530 scanning electron microscope respectively whereas optical absorption data were taken by SHIMADZU UV-240 double-beam spectrophotometer for measurement of optical band gap.

3.3. 2.3. RESULTS AND DISCUSSION

Figure 3.29 shows the XRD patterns of Cu_2S thin films at baking temperature of 400° C, 500° C. Cu_2S peaks are identified from the ASTM data file and shown in table 3.4. A few peaks of CuO also arise in this spectra. Probably some of the copper is oxidised to CuO at this high temperature. The films prepared at the other two baking temperature (360° C & 400° C) are amorphous in nature. A typical scanning electron micrographs of Cu_2S film at 500° C is shown in figure 3.30.

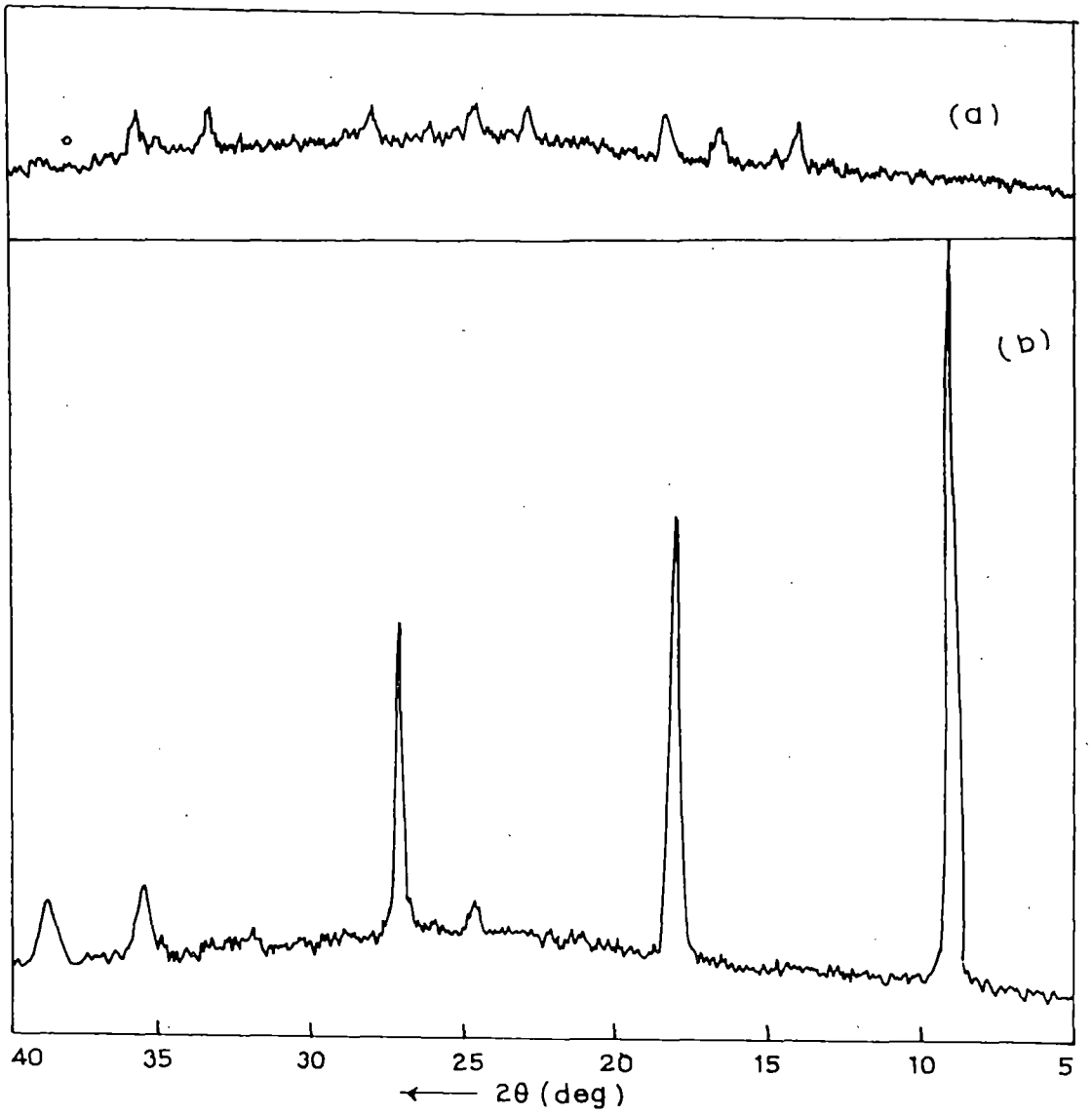

Figure 3.29. X-ray diffractogram of Cu_2S thin films deposited on glass substrate at two different baking temperature [(a), 400° C; (b), 500° C]

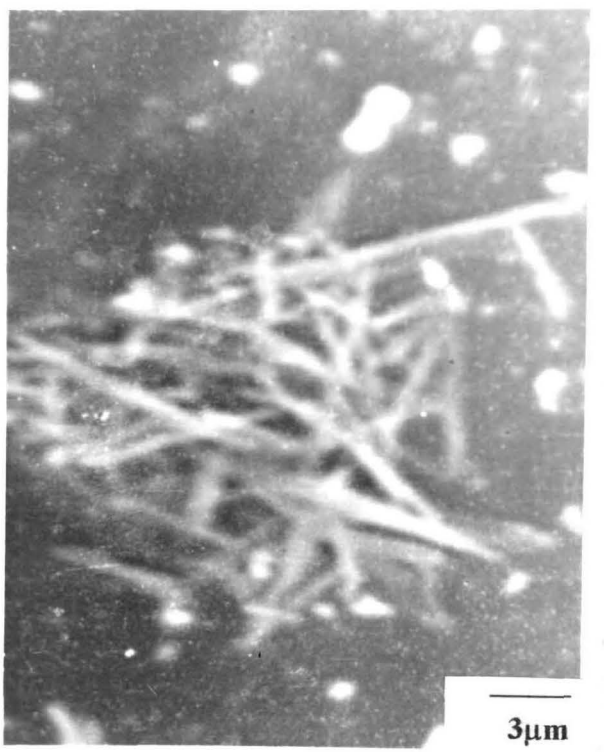

Figure 3.30. A typical scanning electron micrograph of Cu_2S thin film deposited on glass substrate at 500° C

Table - 3.4. Prominent peak position (2θ values) of x-ray diffraction peaks, corresponding d-values and their identification for Cu_2S film.

OBSERVATION			*COMPARISON WITH JCPDS DATA FILE NO. 23-961*		*hkl*
Peak position (2θ)	Observed d- values (A°)	Intensity (I/I_0)	Comparable d- values (A°)	Intensity (I/I_0)	
24.80	3.59	16	3.59	16	162, 203
27.00	3.30	57	3.31	25	322
35.70	2.51	19	2.52	40	$0\underline{1}02^{+}$
38.80	2.32	17	2.32	40	$2\underline{1}02, 471^{+}$

Figure 3.31 shows the optical absoption of Cu_2S films deposited on glass substrtate. The value of the band gap, Eg was determined in the usual way from the intercept of the $(\alpha h\nu)^2$ versus hν plots (fig.3.32) which was a straight line on the hν axis. The optical band gap obtained from this curve is about 1.4 eV. This value is good agreement with the value obtained by other workers [79].

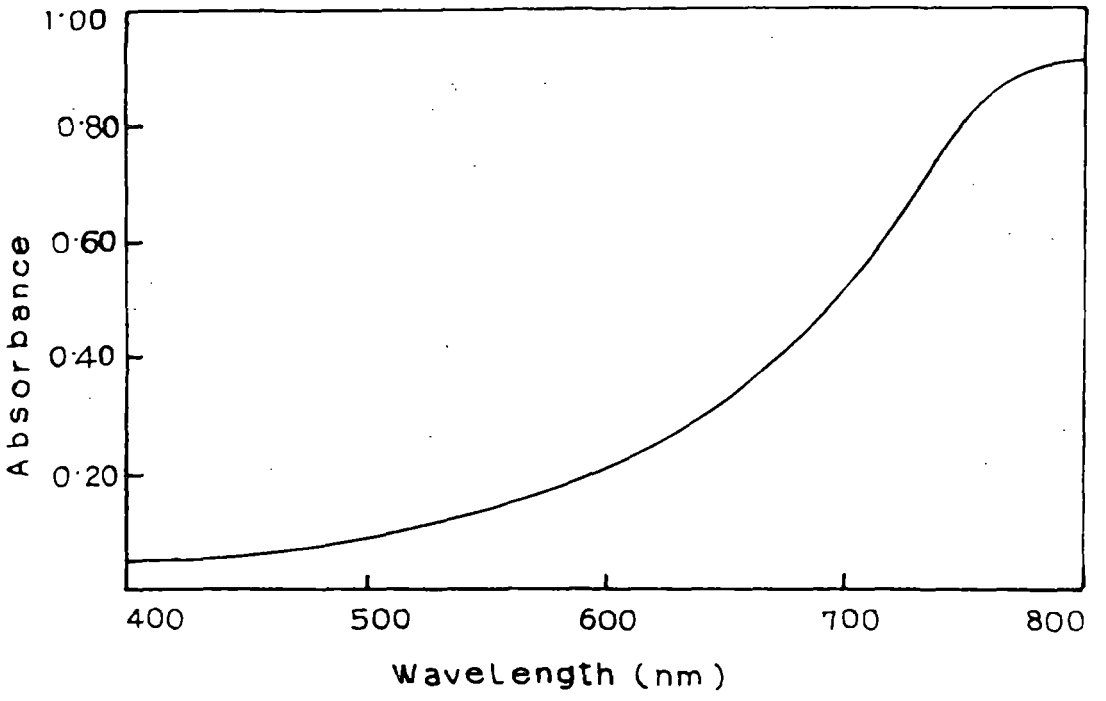

Figure 3.31. Optical absorption spectra of Cu_2S thin films deposited on glass substrate at 400° C.

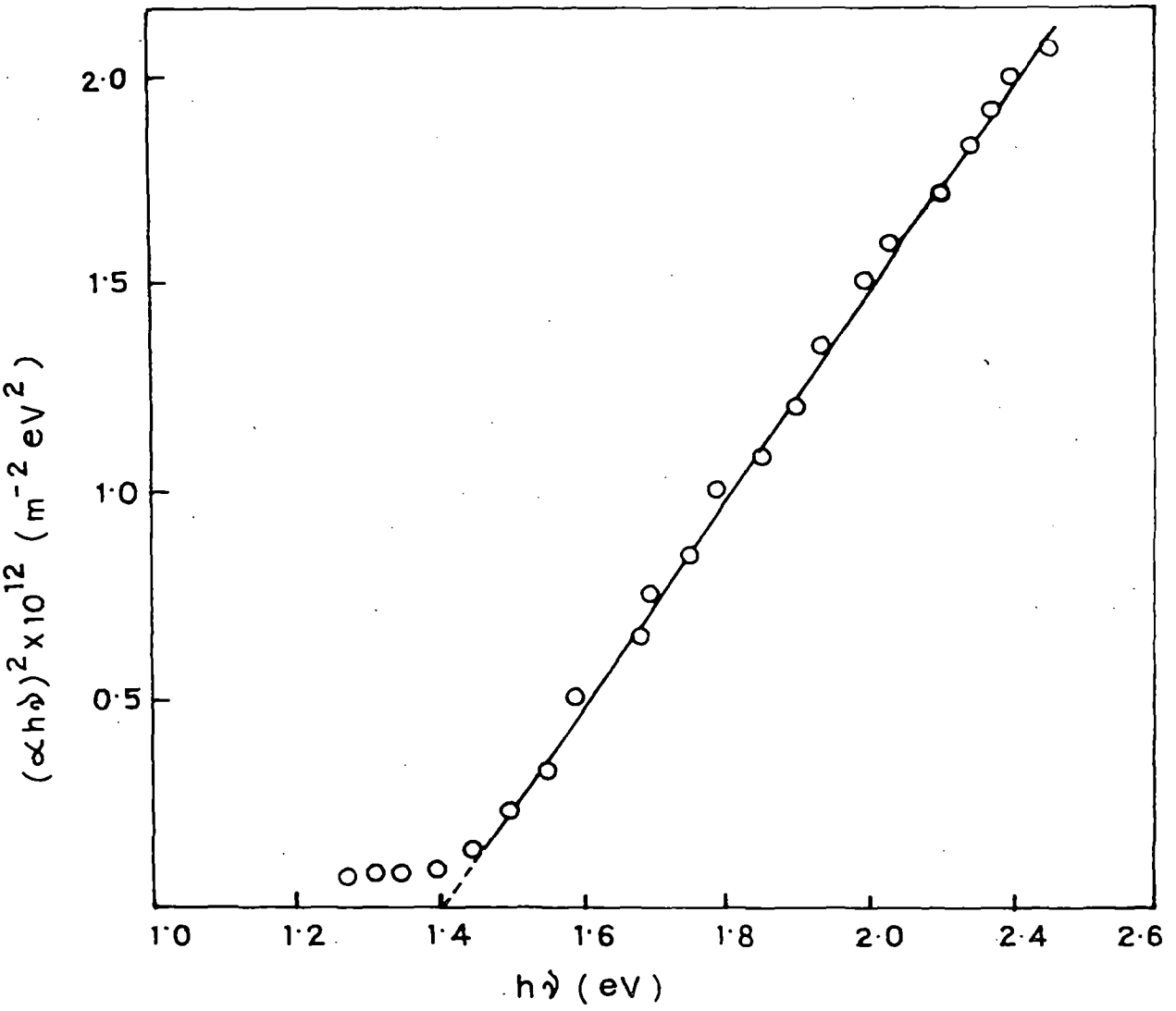

Figure 3.32. Plots of $(\alpha h\nu)^2$ against hν curves of Cu_2S thin film.

3.4. CONCLUSION

Dip technique is a simple and suitable method of obtaining adherent, specular, homogeneous and stoichiometric sulphide thin solid films. In this present chapter, we have prepared successfully a number of sulphide films which may be used in solid state devices. All these films are smooth, uniform and have the usual crystal structure for these materials.

$Zn_xCd_{1-x}S$ ($0 \leq x \leq 0.6$) films were hexagonal in structure, whose lattice parameter ***c*** and ***a*** were found to decrease with increase in x. An increase in x also produces a similar drop in the thickness of the film, the total number of (Cd + Zn) moles in the starting solution remaining constant. This agrees well with the fact that the Zn atoms have a relatively smaller size compared to Cd atoms. The bandgaps obtained from optical absorption and spectral response of photoconductivity measurements are in good agreement with each other and vary from 2.30 eV (CdS) to 2.69 eV ($Zn_{0.6}Cd_{0.4}S$), beyond which the bandgaps obtained from optical absorption measurements (optical bandgap) are much less than that obtained from photoconductive measurements owing to the films becoming amorphous over this range. Surface morphology study by SEM as well as XRD data show that good crystallinity is obtained upto a zinc atomic fraction of 0.4.

SnS ans SnS_2 thin film shows good crystalline structure when prepared at a baking temperature of 300° C for SnS and 360° C for SnS_2 films. Bandgaps obtained from photoconductivity measurements are 1.4 eV and 2.4 eV for SnS and SnS_2 films respectively. Optical absorption measurements on SnS_2 films also yield a value of 2.4 eV. Antimony-doping of SnS_2 films produces an increase in bandgap along with a sharp reduction in crystallinity.

Annealing in air at 400° C both SnS and SnS_2 films convert them to transparent conducting tin dioxide, thus providing an alternative route for its preparation.

MoS_2 thin films show a crystalline structure for a baking temperature of 360° C and 450° C, whereas at 300° C these are amorphous in nature. Optical absorption data shows the films are uniform and homogeneous. The optical bandgap, which was calculated from the absorption data, is 1.80 eV and is comparable with the literature value.

Cu_2S thin films have crystalline structure when the baking temperature was 500° C but has some CuO present because of the oxidation at this high temperature. Optical bandgap, calculated from optical absorption data is 1.4 eV, which is again in agreement with that obtained by other workers.

REFERENCES

1. Y. Endo and T. Taguchi, 1989 *Proc. Mater. Res. Soc.*, Boston,
2. S.Y. Yin, A. L. Fahrenbruch and R.H. Bube 1978 *J.Appl. Phys.* **49** 1294
3. K. T. RamaKrishna Reddy and P. Jayarama Reddy 1992 *J. Phys. D: Appl. Phys.* **25** 1345
4. Kim W. Mitchell, Alan L. Fahrenbruch and Richard H. Bube 1977 *J. of Appl. Phys.* **48** 4365
5. Bulent M. Basol 1984 *J. appl. Phys.* **55** 601
6. Y. K. Jun and H. B. Lm 1988 *J. Electrochem. Society: Electrochemical Science and Technology* **135** 1658
7. Hyeong Soo Kim and Ho Bin Lm 1992 *Thin Solid Films* **214** 207
8. J. Torres and G. Gordillo 1992 *Thin Solid Films* **207** 231
9. Trever A.chynoweth and Richard H. Bube 1980 *J. of Appl. Phys.* **51** 1844
10. T. Yamaquchi, J. Matsufusa and A. Yoshida, 1992 *Jpn. J. Appl. Phys.* **31** L.703
11. T. Walter, M. Ruckh, K. O. Velthaus and H.W. schock, 1992 *Proc. 11th EC Photovoltaic Solar Energy Conf., Montreux,* P.124
12. L. C. Burton and T. L. Hench 1976 *Appl. Phys. Lett.* **29** 612
13. N. Romeo, G. Sberveglieri and L. Tarricone 1978 *Appl. Phys. Lett.* **32** 807
14. O. P. Agnihotri and B. K. Gupta 1979 *Jpn. J. Appl. Phys.* **18** 317
15. R. R. Chamberlin and J. S. Skarman 1966 *J. Electrochem. Soc.* **113** 86.
16. A. Mzerd, D. Sayah, I. J. Saunders and B. K. Jones 1990 *Phys. Stat. Sol. (A)* **119** *487*
17. K. Yamaguchi and S. Sato 1994 *Jpn. J. Appl. Phys.* **23** 126
18. Y.F.Nicolau and J. C. Menard 1988 *J. of crystal growth* ***92*** *128*

19. G. K. Padam, G. L. Malhotra and S. U. M. Rao 1988 *J. Appl. Phys.* **63** 770

20. Y. Sakurai, Y. Kokubun, H. Watanabe and M. Wada 1977 *Jpn. J. Appl. Phys.* **16** 2115

21. S. Yamaga, A. Yoshikawa and H. Kasat 1990 *J. Crystal Growth* **94** 432

22. T. Karasawa, K. Ohkawa and T. Mitsuyu 1991 *J. Appl. Phys.* **64** 3226

23. Takeshi Karasawa, Kazuhiro Ohkawa and Tsuneo Mitsuya 1991 *J. of Appl. Phys* **69** 3226

24.A. Kuroyanagi and T. Suda 1989 *Thin Solid Films* **176** 247

25. A. Kuroyanagi 1990 *J. Appl. Phys.* **68** 5567

26. H. Schroeder. *Oxide layer deposited from organic solutions In G. Hass and R. F. Thun (eds),* 1969 *Physics of Thin Films.* **Vol. 5** Academic Press, New York pp. 87-141

27. C. Terrier, J. P. Chatelon, R. Berjoan and J. A. Roger 1995 *Thin Solid Films* **263** 37

28. M. K. Karanjai and D. DasGupta 1987 *Thin Solid Films* **155** 306

29. JCPDS, Swarthmore, PA Card no. 06 - 0314

30. T. Yamaquchi, Y. Yamamoto, T. Tanaka, Y. Demizu, A. Yoshida 1996 *Thin Solid Films* **281-282** 375

31. R. S. Feigeelson, A. N. Diaye, S. Y. Yin and R. H. Bube 1977 *J. Appl. Phys.* **48** 3162

32. C. M. Mbow, G. W. Cohen-Solal and D. laplaze 1982 Thin Solid Films 87 141

33. R. Hill 1974 *J. Phys C: Solid State Physics* 7 521.

34. K. L. Chopra, R. C. Kainthla, D. K. Pandya and A. P. Thakoorin G. Hass,

M. H. Francombe and J. L. Vossen (eds) 1982 *Physics of thin films* **Vol. 12 Academic Press, New York, P. 167.**

35. W. Albers, C. Hoss, H. I. Vink and I. D. Wassher 1961 *J. Appl. Phys.* **32** 2220.
36. P. M. Nikolic and D. M. Jodoruvic 1986 *J. phys. C. Solid State Physics* **20** 39.
37. M. Sharon, K. Basavaswaran and N. P. Sathe 1985 *J. Sci. Ind. Res.* **44** 593.
38. M. Sharon and K. Basavaswaran 1987 *Solar Cells.* **20** 323.
39. M. Sharon and K. Basavaswaran 1988 *Solar Cells* **25** 91.
40. K. Kawano, R. Nakata and M. Sumita 1989 *J. Phys. D: Appl. Phys.* **22** 136.
41. M. S. Whittingham and A. J. Jacobsen 1982 *Fds. Intercalation Chemistry* **(Academic Press, New York)**
42. W. Hofman 1935 *Z. Kristallogr.* **92** 161.
43. S. Bucchia, J. Jumas and M. Maurir 1981 *Acta Crystallogr. B* **37** 1903.
44. J. Offedol 1928 *J. Phys. Chem.* **134 No. 3/4** 301.
45. D. Mootz and A. Puhl 1967 *Acta Crystallogr.* **23 No.** 3 471.
46. L. D. C. Bok and J. C. A. Boeyens 1957 *J. S. Afric Chem Inst.* **10 No. 2** 49.
47. I. S. Anderson, M. C. Morton 1945 *Proc R. Soc. A* **48** 83.
48. M. Ristov, G. J. Sinadinovski, I. Grozdanov and M. Mttocski 1989 *Thin Solid Films* **173** 53.
49. T. Shibata, Y. Muranushi, T. Miura and T. Kishi 1991 *J. of Material Science* **26** 5107.
50. Zulkarnain Zainal, Mohd Zobir Hussein and Arniza Ghazali 1996 *Solar Energy Materials and Solar Cells* **40** 347.

51. R. Banerjee, Swati Ray and A. K. Barua 1984 *Indian J. Physics* **58** 166.

52. P. K. Nair, M. T. S. Nair, Ralph A. Zingaro and Edward A. Meyers 1994 *Thin Solid Films* **239** 85.

53. W. H. Bauer 1956 *Acta Cryst.* 1 515.

54. H. Tributsch 1980 *Faraday Discuss.* **70** 1.

55. H. Tributsch and J. C. Bennelt 1977 *J. Electroanal.Chem.* **81** 97.

56. T. A. Recoraro and R. R. Chaianelli 1981 *J. Catal.* **67** 430.

57. R. Reichelt and G. Mair 1978 *J. Appl. Phys.* **49** 1245.

58. T. Spalvins 1978 *Thin Solid Films* **53** 286.

59. T. Spalvins 1969 *ASLE Trans.* **12** 36.

60. E. A. Panomarev, M. Neumann-Spallart, G. Hodes, C. Levy-Clement 1996 *Thin Solid Films* **280** 86.

61. J. Moser and F. Levy 1994 *Thin Solid Films* **240** 56.

62. P. Gribi, Z. W. Sun and F. Levy, 1989 *J. Phys. D. Appl. Phys.* **22** 238.

63 H. Dimigen, H. Hubsch, P. Willich and K. Reichelt 1985 . *Thin Solid Films* **129** 79.

64. L.F. Schneemeyer and U. Cohen 1983 *J. Electrochem. Soc.* **130** 1536.

65. N. T. McDevill, J. S. Zabinski and M. S. Donley 1994 *Thin Solid Films* **240** 76.

66. J. S. Zabinski, M. S. Donley, V. J. Dyhouse and M. T. Mcdevitt 1992 *Thin Solid Films* **214** 156.

67. V. Yu. Fominski, A. R. Markeev, V. N. Nevolin, V.B. Prokopenko and A. R. Vrublevski 1994 *Thin Solid Films* **248** 240.

68. E. Bucher, *Photovoltaic properties of solid state junctions of layered Semiconductors, in A. Aruchany (ed), Photoelectro chemistry and Photovoltaics of layered Semiconductors, Kluwer, Dordrecht,* 1992, **pp. 36.**

69. J. J. Loferski,J. Shewehum, S. D. Mittleman , E. A. De Meo, R. Arnott, H. L. Hwang, R. Beauliew and G. Chapman 1979 *Solar Energy Mater.* **1** 152.

70. M. Savelli and J. Bougnot, in B.O. Serophin (ed) 1979 *Solar Energy Conversion: Topic In Applied Physics* **Vol. 31 Springer, Berin** P. 231.

71. K. Okamoto and S. Kawai 1973 *Jpn . J. Appl. Phys.* **12** 1130.

72. S. Couve, L. Gouskov, L. Szepessy, J. Vedel and E. Castel 1973 *Thin Solid Films* **15** 223.

73. I. Grozdanov, C. K. Barlingay, S. K. Dey, M. Ristov and M. Najdoski 1994 *Thin Solid Films* **250** 67.

74. A.F. Well 1962 *Structural Inorganic Chemistry, Clarendon Press, Oxford, 3rd edn.* P. 883.

75. S. Djurle 1958 *Acta Chem. Sand.* **12** 1415.

76. E. Ramli, T. B. Rauchfiuss and C. l. Stern 1990 *J. Am. Chem. Soc.* **112** 4043.

77. H. Fjellvag, F. Gronvold, S. Stolen. A. F. Andersen, R. Mullerkafer and A. Simon 1988 *Z. Kristallogr* **184** 111.

78. B. Rezig, S. Duchemin, F. Guastavino 1979 *Sol. Energy Mater.* **6** 53.

79. H. S. Randhawa, R. F. Bunshah, D. G. Brock, B. M. Basol and O. M. Staffsudd 1982 *Sol. Energy Mater.* **6** 445.

80. R.N. Bhattacharya and P. Pramanic 1981 *Bull Mater Sci.* **3** 403.

81. M. T. S. Nair and P. K. Nair 1989 *Semicon. Sci. Technol.* **4** 191.

82. K. M. Gadave and C. D. Lokhande 1993 *Thin Solid Films* **229** 1.

83. M. Inoue, C. Cruz-Vazquez, M. B. Inoue, K. B. nebesny and Q. Fernando 1993 *Snthetic Metals* **55-57** 3748.

84. Takakazu Yamamoto, Kuniaki Tanaka, Etsuo Kubota and Kohtaro Osakada 1993 *Chem. Mater.* **5** 1352.